Consistency of Spatiotemporal Variability of MODIS and ERA5-Land Surface Warming Trends over Complex Topography

Meric Yilmaz

Department of Civil Engineering, Atilim University, Ankara, Turkey

Email: meric.yilmaz@atilim.edu.tr

ORCID: 0000-0001-6921-7687

Acknowledgments: The author would like to thank to MGM for providing the daily mean temperature data of all meteorological stations of Turkey. The author also thanks to ECMWF for publicly available ERA5-Land datasets and NASA for publicly available MODIS and SRTM datasets.

Abstract

In this study, the trend of widely used MODIS MxD11 and MxD21 Land Surface Temperature (LST) and ERA5-Land Skin Temperature (SKT) and 2m air temperature products were validated using 2m air temperature trends obtained by ground observations from 266 stations in 2000–2021 over Turkey, known to have complex topography. The results show that colder regions have substantially higher temporal temperature variability than warmer ones. MxD21 and MxD11 products are 4.4 °C and 2.9 °C warmer than ERA5-Land products, respectively, while ERA5-Land products (SKT and 2m) have nearly similar averages (12.5 °C). The consistency between MODIS and ERA5-Land data is significantly lower over areas with more complex topography and irrigation activities, despite the fact that the products show a high linear relationship over the study area. While February trends are consistently much higher than other months (2.2 and 1.4 °C/decade for MODIS and ERA5-Land, respectively), overall MODIS skin temperature products (0.7 °C/decade) generally exhibit smaller trends than ERA5-Land skin and air temperature trends (0.94 °C/decade). The results suggested that MODIS and ERA5-Land trends, which are highly consistent with observations, might replace observations in the absence of long-term station-based records.

Keywords: Surface temperature; warming trend; MxD11; MxD21; ERA5-Land.

1 Introduction

One of the most significant indicators of climate change is surface temperature, and the following definition of surface temperature is consistent with that in (IPCC 2021a): Land surface temperature (LST), also known as skin temperature (SKT), is the theoretical skin

temperature (i.e., depending on the application, top few cm of the surface) of the Earth and is a key component in surface energy and water balance estimation at regional and global scales (Friedl 2002). On the other hand, estimates of near-surface air temperature (i.e., at 2 m level) are pertinent to estimates based on numerical weather prediction (NWP) models and ground station-based measurements. While the characteristics of the two estimates of surface temperature—LST/SKT and 2m air temperatures—are distinct, especially at short time scales (like hourly), they are both impacted by the changing climate at long time scales. All of ground station-, satellite remote sensing-, and NWP model-based frameworks can be used to retrieve LST/SKT and air temperature. Among them, while air temperature estimates are more commonly obtained through ground station-based observations and NWP, LST/SKT datasets used in the literature are often obtained utilizing satellite-based remote sensing (Yao et al. 2017, 2019; Reiners et al. 2023).

Accurate surface temperature estimation is essential since it is one of the most significant markers of climate change and has drastically increased after the pre-industrial age of 1850–1900. The Intergovernmental Panel on Climate Change states that the rate of increase in surface temperature has accelerated since 1970 (IPCC 2021a). Increased mortality rates, urban heat islands, and drought intensity and duration are all indicators of rising surface temperatures (Basu and Samet 2002; Imhoff et al. 2010; Manesh et al. 2019). The increase in surface temperature brought on by climate change is not uniform across the continents, though, as there are hotspot locations on Earth. Europe and the Mediterranean Basin, for instance, see greater increases in mean temperatures, intensity, and frequency of hot extremes

than other regions, according to ample evidence of climate change (IPCC 2021a, b; Cos et al. 2022). Furthermore, land surface heterogeneity, particularly in complex topography, causes fast spatial and temporal fluctuations in surface temperature (Li et al. 2013).

Estimations of the surface temperature are employed in a wide range of research, including but not limited to those pertaining to meteorology, climatology, hydrology, and public health (Duan et al. 2014, 2017). Consequently, in order to have a better understanding of the spatio-temporal rising of surface temperature, it is required to precisely determine the current rate of increase of surface temperature under changing climate.

One of the most widely utilized LST products among the satellite-based products is offered by the Moderate Resolution Imaging Spectroradiometer (MODIS) (Wan 2019). Due to its high accuracy estimation of the LST with a global coverage, MODIS LST product is extensively employed in studies at both regional and global scale (Pepin et al. 2019; Zhao et al. 2019; Reiners et al. 2021; Wang et al. 2022). MODIS LST product has been also used in estimation of air temperature (Zhang et al. 2016; Yang et al. 2017) provided that LST and air temperature have strong correlation (Mildrexler et al. 2011; Benali et al. 2012). However, in order to fully understand this link, a detailed comparison is necessary since their variability patterns may vary, particularly in mountainous regions (Pepin et al. 2016, 2019; Aguilar-Lome et al. 2019). Although MODIS has been monitoring LST successfully since 2000, explicit intercomparison of MODIS-based surface skin temperature trends against observation-based trends (Liu et al. 2022; Recondo et al. 2022) over complex topography has not been done (i.e., can MODIS LST trends replace observation-based air temperature

75 trends?). Additionally, there are two different flavors of MODIS LST products, namely
76 MxD11 and MxD21; yet their explicit validation and intercomparison (Yao et al. 2020) are
77 required to fully understand their nature and the impact of the variations in their algorithms on
78 temperature estimates.

79 NWP models offer users spatially and temporally continuous SKT and 2m air
80 temperature datasets as an alternative to remote sensing-based products, that may represent
81 conditions from almost a century or earlier. Among the alternatives, perhaps ERA5-Land
82 (Muñoz-Sabater et al. 2021) offers one of the most recent but accurate products (Yilmaz
83 2023). Here, skin layer represents the vegetation layer, the top layer of the bare soil/snow
84 pack (ECMWF 2016), where ERA5/ERA5-Land of ECMWF offer very accurate estimates of
85 both SKT and air temperature. Yet, to improve the simulation accuracy of climate models and
86 provide retrieval strategies for soil and vegetation moisture, very precise SKT and 2m
87 temperature values must be retrieved (Liu et al. 2022). On the other hand, limited number of
88 studies have explicitly validated the ERA5-Land and ERA5 temperature trend accuracies
89 (Yilmaz 2023), and the accuracy of SKT trends generated using ERA5-Land against remote
90 sensing-based estimates (e.g., MODIS) has not explicitly been inter-compared.

91 Complex topography poses challenges to both satellite- and NWP-based retrievals,
92 where the accuracy over complex topography is often lower than in non-complex regions
93 (Amjad et al. 2020). Hence, it is necessary to explicitly evaluate the accuracy of LST/SKT
94 and 2m temperature trends over complex regions. Known for its very complex terrain, Turkey
95 is also a climate change hot spot (Amjad et al. 2020; Bagcaci et al. 2021). While studies

performed over Turkey have focused on the validation of the temperature datasets (Bagcaci et al. 2021; Yilmaz 2022) and NWP-based air temperature validation (Yilmaz 2023), remote sensing-based LST trend investigation and validation has not been performed over Turkey before.

In this study, for the first time, validation of MODIS LST trends, intercomparison of two different MODIS LST product flavors (MxD11 and MxD21), and intercomparison of MODIS LST and ERA5-Land SKT/2m temperature trends were made over a complex terrain. Also, for the first time, the trends of these four products were explicitly intercompared against ground station observation-based temperature trends. Following the dataset and methodology introduction in section 2, the results are presented in section 3 and discussed in section 4, and the conclusions are given in section 5.

2 Materials and Methods

2.1 Study Area

This study is performed over Turkey located in the Mediterranean Basin and considered to be a climate change hotspot region (IPCC 2021b). With a 783,562 km^2 surface area, Turkey's elevation ranges from 0 to 5137 m, and it has a complex topography variability (Amjad et al. 2020). It also has a significant degree of climatic variety, with a predominance of temperate and subtropical climate zones (Eken et al. 2008). Köppen-Geiger climate classification map of Turkey for 1980–2016 is presented in Fig. 1. The map is retrieved from the study of Beck et al. (2018). The datasets for this study were initially collected throughout a region bounded by longitudes 25° E to 45° E and latitudes 35° N to 43° N; they were later

117 trimmed using Turkey's borders. In this study, analyses were conducted over seven
118 geographic regions of Turkey (Yilmaz 2023), including I-Marmara (MAR), II-Aegean (AEG),
119 III-Mediterranean (MED), IV-Central Anatolia (CE-ANA), V-Black Sea (BL-SEA), VI-
120 Eastern Anatolia (EA-ANA), and VII-South Eastern Anatolia (SE-ANA).

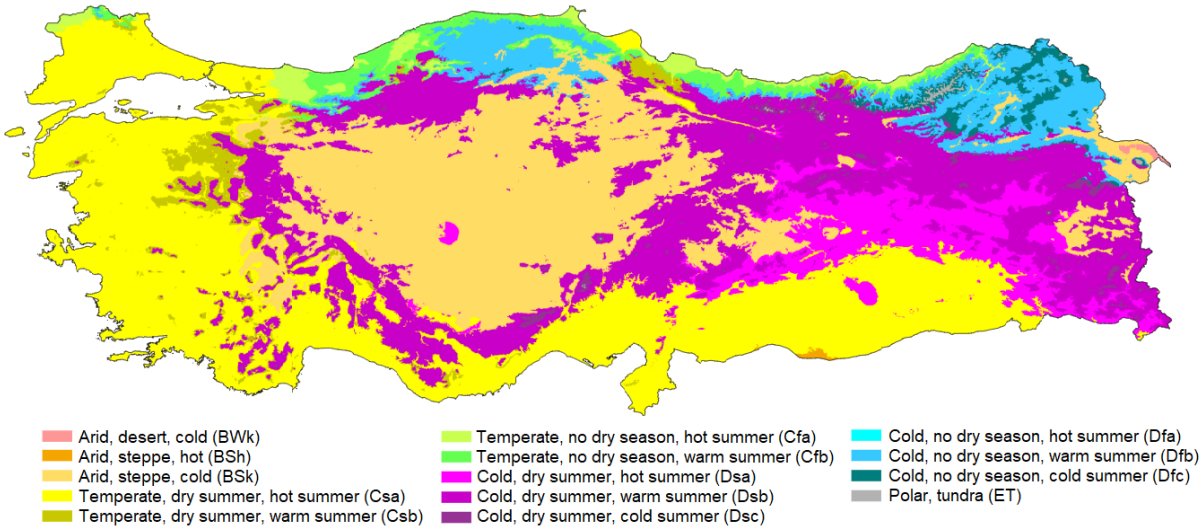

121

122 **Fig. 1** Köppen-Geiger climate classification map of Turkey for 1980–2016 period. The map is
123 retrieved from Beck et al. (2018)

124 **2.2 Datasets**

125 Monthly ground station-based 2m air temperature observations, monthly ECMWF
126 ERA5-Land SKT and 2m air temperature datasets, and monthly MODIS LST datasets MxD11
127 and MxD21 were all used in this investigation (Table 1). Datasets from MODIS and ERA5-
128 Land were obtained globally at monthly temporal resolution; datasets that fell within Turkey's
129 border were then cropped. While station-based observations were initially collected with a
130 daily temporal resolution, they were later averaged out to have a monthly resolution. These
131 datasets of monthly average temperatures are used in all the analyses conducted in this study.

Despite the fact that ERA5-Land and a number of station observations cover a wider time span, this study focuses on the period from 2000 to 2021 due to the availability of MODIS LST data. Below are further details about these products.

Table 1 Characteristics of the datasets utilized in this study

Product Name (Abbreviation)	Spatial / Temporal Resolution	File Format	Data Availability (in 2000-2021)	Source
MOD11C3.061 LST (M11 Ts)	0.05° Monthly	HDF	Feb 2000 – Dec 2021	MODIS Terra – Satellite https://e4ftl01.cr.usgs.gov/MOLT/MOD11C3.061/ (Accessed on 14 December 2022)
MOD21C3.061 LST (M21 Ts)	0.05° Monthly	HDF	Feb 2000 – Dec 2021	MODIS Terra – Satellite https://e4ftl01.cr.usgs.gov/MOLT/MOD21C3.061/ (Accessed on 14 December 2022)
MYD11C3.061 LST (M11 Ts)	0.05° Monthly	HDF	Jul 2002 – Dec 2021	MODIS Aqua – Satellite https://e4ftl01.cr.usgs.gov/MOLA/MYD11C3.061/ (Accessed on 14 December 2022)
MYD21C3.061 LST (M21 Ts)	0.05° Monthly	HDF	Jul 2002 – Dec 2021	MODIS Aqua – Satellite https://e4ftl01.cr.usgs.gov/MOLA/MYD21C3.061/ (Accessed on 14 December 2022)
ERA5-Land SKT (E5L Ts)	0.10° Monthly	NetCDF	Jan 2000 – Dec 2021	ECMWF – Reanalysis https://cds.climate.copernicus.eu/ (Accessed on 5 August 2022)
ERA5-Land 2m (E5L Ta)	0.10° Monthly	NetCDF	Jan 2000 – Dec 2021	ECMWF – Reanalysis https://cds.climate.copernicus.eu/ (Accessed on 5 August 2022)
Station 2m (STA Ta)	Point Daily	TXT	Jan 2000 – Dec 2021	MGM – Observation https://mevbis.mgm.gov.tr/ (Sent by MGM on 25 April 2022)
Slope (S)	1 km	GeoTiff	–	SRTM – Satellite https://www.earthenv.org/topography (Accessed on 1 June 2022)
Elevation (DEM)	1 km	GeoTiff	–	SRTM – Satellite https://www.earthenv.org/topography (Accessed on 1 June 2022)

2.2.1 MODIS Land Surface Temperature (M11 Ts and M21 Ts)

Data on land surface temperatures used in this study were gathered by the MODIS instrument installed on the National Aeronautics and Space Administration's (NASA) Terra and Aqua sun-synchronous and near-polar orbiting satellites. Here, Terra (EOS AM-1) and Aqua (EOS PM-1) make equatorial passes at 10:30 am/pm and 1:30 am/pm, respectively.

LST datasets were collected from MxD11 and MxD21, two separate MODIS products. To retrieve LST, the MxD11 utilizes the split-window algorithm and the day/night algorithm. The monthly Climate Modeling Grid (CMG) products MOD11C3.061 (Terra) and MYD11C3.061 (Aqua) (Wan 2019), collectively referred to as MxD11, were used in this study. The monthly CMG LST products MOD21C3.061 (Terra) and MYD21C3.061 (Aqua) from Collection 6.1 (Hulley et al. 2022) were also utilized, where these products in this study are referred to as MxD21. The Temperature and Emissivity Separation (TES) technique is utilized by the MxD21 product to dynamically retrieve LST. All four products were downloaded in HDF format at 0.05° spatial resolution (~5600 km at the equator) from NASA's Land Processes Distributed Active Archive Center (LP DAAC) website (NASA). By averaging all available monthly MOD11C3.061 and MYD11C3.061 datasets (both daytime and nighttime) for each month separately during the study period, the monthly mean MxD11 dataset was calculated. Similarly, monthly MOD21C3.061 and MYD21C3.061 datasets were averaged to create the monthly mean MxD21 dataset. All Terra (MOD) and Aqua (MYD) monthly products (MOD11C3.061, MYD11C3.061, MOD21C3.061, and MYD21C3.061) are continuous and do not contain any missing monthly record between July 2002 until December 2021 (i.e., end of the study period). Accordingly, no gap-filling algorithm, that are commonly utilized to fill in the gaps in daily or 8-day datasets (Yao et al. 2021, 2023), is used in this study. While Aqua (MYD11 and MYD21) datasets do not have any data between February 2000 and June 2002, Terra (MOD11 and MOD21) monthly products are continuous and available. Here, in this study, for the sake of utilizing longer records, MxD11 and MxD21

datasets between February 2000 and June 2002 were only taken from Terra-based products, while remaining ~20 years were obtained utilizing both Terra- and Aqua-based products. In this study, MxD11 LST and MxD21 LST are denoted by M11 Ts and M21 Ts, respectively. Here, All MODIS datasets (from Aqua and Terra during day and night) are averaged to obtain a single representative temperature estimate for each month.

2.2.2 ERA5-Land Skin Temperature (E5L Ts) and 2m Air Temperature (E5L Ta)

ERA5-Land (Muñoz-Sabater et al. 2021) by ECMWF is the latest global dataset for the land component of the fifth-generation reanalysis product ERA5. ERA5-Land provides 50 variables that describe water and energy cycles over the land globally with a horizontal resolution of 0.10° x 0.10° (~9 km) (CDS; Muñoz-Sabater et al. 2021; Stefanidis et al. 2022). ERA5-Land datasets are continuously available from 1950 to the present in ECMWF Climate Data Service (CDS) in NetCDF format, with an hourly to monthly temporal resolution (CDS). The monthly ERA5-Land air temperature data on single levels—which represent the near-surface temperature—and the skin temperature (SKT) data—which represent the LST—are the two variables used in this study. SKT represents the top 7 cm of the surface layer of the ECMWF's land surface model, Carbon Hydrology-Tiled ECMWF Scheme for Surface Exchanges over Land (CHTESSEL). The monthly ERA5-Land 2m air temperature datasets and SKT datasets for 2000–2021 period that were used in this study were downloaded on 19 November 2022. In this study, ERA5-Land SKT and ERA5-Land air temperature are denoted by E5L Ts and E5L Ta, respectively.

2.2.3 Ground Station-Based 2m Air Temperature Observations (STA Ta)

The General Directorate of Meteorology (MGM) provided daily ground station-based near-surface temperature measurements for Turkey. The temperature data were provided by MGM on request. Over time, the number of operational meteorological stations expanded to more than 2500 stations throughout Turkey (MGM). However, there are discontinuities in the observations collected by the stations; newly established stations have shorter observation records than MODIS datasets. Some of the formerly established stations are no longer operational, or no proper data have been collected in certain months. Accordingly, a standard was set in this study which disqualifies stations with less than 95% of the data collected between 2000 and 2021. 266 stations out of all the stations were selected for this study since they had more than 95% of the temperature data collected throughout the study period. For the analysis, monthly mean temperature datasets were created by averaging daily temperature readings.

Ground station-based observations are acquired at 2 m height, while there are no land surface temperature observations in Turkey by MGM. Skin temperature measurements are taken at a small number of sites that do not consistently and densely cover the entire research region. As a result, this study only has access to and uses ground station-based near-surface temperature observations. In this study, station-based 2m air temperature observations are denoted by STA Ta.

2.2.4 Slope, Elevation, and Station Density

The study area has very complex topography in relation with its rapidly changing slope characteristics. Here, in this study, the variability of trends obtained from ERA5-Land and MODIS products with respect to changing topographical complexity is investigated. Accordingly, the stations are grouped into two classes: non-complex and complex. As the definitions of complex topography in different studies changes, here the definition of Amjad et al. (2020), that the terrains with slopes less than 5% are considered as non-complex, is employed, whereas slopes greater than 5% are regarded as complex. In this study, the slope (S) and elevation (DEM) data were obtained from 1 km mean datasets from NASA's Shuttle Radar Topography Mission (SRTM) in GeoTiff format (Amatulli et al. 2018). Later the percent slope values were extracted over the locations of individual stations by utilizing the values of the grids that contains the stations.

Among the regions, BL-SEA and AEG have the highest and the lowest average slope (%), respectively, while EA-ANA and MAR has the highest and the lowest average elevation above mean sea level, respectively (Table 2). Among the regions, AEG and EA-ANA have the highest and the lowest station density, respectively. While EA-ANA has the largest area among the regions, it has the lowest station density. Overall, the regions with relatively lower slope (MAR, AEG, SE-ANA) has higher station density than higher slope (MED, CE-ANA, BL-SEA, EA-ANA), where the station density changes more with slope than elevation.

Table 2 Geographical characteristics of ground station density of the study area (TR) and seven geographical regions of Turkey

Region	Area (km^2)	S (%)	DEM (m)	Total # of stations	Area in km^2 per station	Station per 1000 km^2 area
TR	784000	3.35	694	266	2947	0.34
MAR	65000	2.81	186	38	1711	0.58
AEG	83000	2.32	350	51	1627	0.61
MED	114000	3.05	403	36	3167	0.32
CE-ANA	162000	3.12	1081	45	3600	0.28
BL-SEA	134000	4.85	389	37	3622	0.28
EA-ANA	165000	4.01	1379	23	7174	0.14
SE-ANA	61000	3.22	799	36	1694	0.59

2.3 Analyses

2.3.1 Dataset Spatial Resolution

Datasets that were utilized in this study have different spatial resolution. MODIS and ERA5-Land are gridded datasets with 0.05° and 0.10° spatial resolution, respectively, while the MGM station-based datasets are point observations. To ensure the comparisons between the statistics of different datasets are done objectively, the spatial and the temporal resolution of the products should be the same. Accordingly, this disparity between the spatial resolutions of the gridded MODIS and ERA5-Land datasets was eliminated before any further analysis to be performed in this study. This is achieved by averaging the values of MODIS pixels that fall inside ERA5-Land pixels. Thus, MODIS and ERA5-Land datasets with a spatial resolution of 0.10° were acquired for the area delimited by 35°N and 43°N and 25°E and 45°E, respectively. Accordingly, gridded maps have 201 columns and 81 rows, total 16,281 grids. On the other hand, only 8,110 grids cover the study region, and the remaining grids were not used in the analyses of this study. For all of the analyses in this study, these datasets that have the same spatial (i.e., 0.10°) and temporal (i.e., monthly) resolutions were utilized.

Additional analyses that serve as the foundation for the direct evaluation of gridded MODIS and ERA5-Land datasets use station-based point observations as the ground truth. Each station's MODIS and ERA5-Land grids were retrieved for these analyses. This enabled it possible to compare station-based observations to the equivalent MODIS and ERA5-Land data on an individual basis.

2.3.2 Data Homogeneity

Any analysis in this study was carried out if the temperature data are mutually available for all products in purpose of homogeneous intercomparison of MODIS, ERA5-Land, and station-based datasets. Therefore, in case any product has no available data over any grid and/or month, then other products were removed from the analyses for the relevant grid and/or month.

2.3.3 Map-Based and Point-Based Analyses

MODIS and ERA5-Land are gridded products and observations collected over stations are point-based values. Accordingly, analyses were performed using product values for both entire grids and only over stations. Here, analyses using data from all grids are referred to as "map-based," while analyses using data from only grids with ground stations are referred to as "point-based." For instance, for the map-based estimate, the mean temperature over the whole study region was derived using data from gridded products over all 8,110 grids, while for the point-based estimate, only values from the 261 grids containing the 266 stations were used. Here five grids contain multiple stations, while for these five stations same grid values of four products were assigned as the pair of the station data. Along with evaluations of the entire

research region, in-depth investigations were carried out separately over each geographical area. Here, the map- and point-based analyses were also made using the relevant grids that fall inside each geographic region separately. For the seven regions specified under section 2.1, values retrieved over a total of 771, 921, 901, 1937, 1259, 1476, and 848 grids (total 8,110) were utilized for MAR, AEG, MED, CE-ANA, BL-SEA, EA-ANA, and SE-ANA regions, respectively, for the map-based analyses. On the other hand, 36, 38, 37, 51, 36, 45, and 23 stations (total 266) and the representative grids located in MAR, AEG, MED, CE-ANA, BL-SEA, EA-ANA, and SE-ANA regions, respectively, were utilized for the point-based analyses.

2.3.4 Temperature Statistics

Mean, standard deviation, and trend of several monthly datasets were calculated separately for each product over each region (total of seven regions) and month (total of 12 months). Additionally, similar analyses were also performed using all values retrieved for all months and over 8,110 grids for map-based and 261 grids for point-based investigations. For example, for the map-based analyses over MAR region, temporal mean, standard deviation, and trend were calculated utilizing the temperature values for 12*22 months for each grid (totaling 771 grids); these statistics were then averaged to produce a region-representative value for each statistic. Similar calculations were made for the point-based estimates; mean, standard deviation, and trend statistics were calculated for each grid representing each station that fell within the relevant region separately (for instance, 36 stations for MAR region), and

then these different estimates representing each station were averaged out to produce a single value for each statistic for each region.

Linear regression-based trends (°C/decade) were calculated for each monthly product for the whole study period of 2000-2021. Among this 264 months of data, 240 months of minimum data availability was enforced for the calculation of trends; if the length of mutually available datasets was shorter for any grid, then trends were not calculated the trends were assigned as missing for relevant grids and stations. Here, all 8,110 grids have at least 240 available datasets, accordingly, trends were calculated for all grids inside entire study region.

In monthly and regional analyses, correlation between the temperature products was calculated in addition to the mean, standard deviation, and trends (i.e., for 12 months and seven regions separately). In this study, the correlations were calculated from the anomaly time series, where the monthly seasonality was removed from the total time series. Here, the anomaly time series were created because the dominant seasonality, rather than anomaly, controlled the correlations of the whole time series, making the consistency between the anomaly components more intriguing than the cyclic seasonality information.

2.3.5 Temperature Difference Statistics

To study the regional and/or temporal patterns present in the disparities between the products, statistics (mean, standard deviation, and trend) of temperature differences were also calculated, similar to the statistics obtained utilizing temperature values. These temperature difference-based statistics were only performed map-based but not point-based for brevity. Here, the differences for six different data pairings were calculated. The second data in each

pair was subtracted from the first in the following pairs: 1) M11 Ts – M21 Ts, 2) M11 Ts – E5L Ts, 3) M11 Ts – E5L Ta, 4) M21 Ts – E5L Ts, 5) M21 Ts – E5L Ta, and 6) E5L Ts – E5L Ta.

3 Results

Intercomparison and investigation of monthly MODIS LST (M11 Ts and M21 Ts) and ERA5-Land SKT and 2m air temperature (E5L Ts and E5L Ta) products between 2000 and 2021 were performed over Turkey, while validation of these datasets were made via 2m air temperature observations (STA Ta) acquired at 266 ground stations. Both map-based (i.e., using all data retrieved from maps) and point-based (i.e., using only datasets acquired from the grids containing ground-based stations) analyses performed in this study used mutually available datasets; if any product was not available over any grid and/or month, then other products were removed from the analyses for the relevant grid and/or month.

3.1 Mean, Standard Deviation, and Trend of Temperature Products

Average temperatures of these four map-based temperature products over entire Turkey are shown in Fig. 2 and Tables 2 and 3 presents the statistics of these map-based temperature products. On average, as shown in Table 3, MODIS products (13.51 and 15.02 °C for M11 Ts and M21 Ts, respectively) are warmer than ERA5-Land products (11.07 and 11.12 °C for E5L Ts and E5L Ta, respectively). The highest mean temperature values are found in M21 Ts; which is 1.51, 3.95, and 3.90 °C warmer than M11 Ts, E5L Ts, and E5L Ta, respectively (Table 3). The mean temperatures are lowest in the snow-dominated EA-ANA region and greatest in the SE-ANA region. The four products' average temperatures for these

two regions varied by 8.4 °C (Table 3), with a 26 °C difference between the long-term average temperatures of the warmest and coldest regions (i.e., the range of temperature values given in Fig. 2).

Table 3 Spatial variability of map-based statistics of M11 Ts, M21 Ts, E5L Ts, and E5L Ta products over the study area (TR) and seven geographical regions of Turkey utilizing monthly datasets between 2000 and 2021.

Map-based Statistics	Products	Regions							
		TR	**MAR**	**AEG**	**MED**	**CE-ANA**	**BL-SEA**	**EA-ANA**	**SE-ANA**
Mean (°C)	M11 Ts	13.51	14.86	16.00	15.51	13.52	11.14	9.38	18.24
	M21 Ts	15.02	16.49	17.42	17.00	15.03	12.81	10.84	19.64
	E5L Ts	11.07	13.78	13.85	13.53	10.81	8.78	6.55	14.97
	E5L Ta	11.12	13.61	13.86	13.23	10.48	9.12	7.30	14.87
Standard Deviation (°C)	M11 Ts	10.47	8.31	9.35	9.41	10.96	8.96	12.87	11.74
	M21 Ts	10.78	8.43	9.54	9.75	11.29	9.06	13.56	11.89
	E5L Ts	9.86	8.09	8.98	9.26	10.27	9.01	11.15	11.08
	E5L Ta	8.47	7.26	7.89	7.93	8.57	7.65	9.53	9.84
Anomaly Correlation	M11 Ts&M21 Ts	0.95	0.94	0.96	0.95	0.96	0.95	0.95	0.96
	M11 Ts&E5L Ts	0.82	0.85	0.84	0.82	0.86	0.84	0.78	0.76
	M11 Ts&E5L Ta	0.84	0.85	0.85	0.85	0.85	0.86	0.83	0.79
	M21 Ts&E5L Ts	0.81	0.82	0.83	0.82	0.84	0.82	0.77	0.77
	M21 Ts&E5L Ta	0.82	0.82	0.83	0.84	0.83	0.84	0.81	0.80
	E5L Ts&E5L Ta	0.96	0.98	0.98	0.96	0.96	0.96	0.93	0.96
Trend (°C/decade)	M11 Ts	0.66	0.42	0.37	0.59	0.71	0.68	1.00	0.50
	M21 Ts	0.74	0.41	0.40	0.68	0.82	0.72	1.15	0.63
	E5L Ts	0.96	0.75	0.84	0.94	0.97	1.00	1.08	0.97
	E5L Ta	0.92	0.73	0.83	0.88	0.89	0.97	1.07	0.95

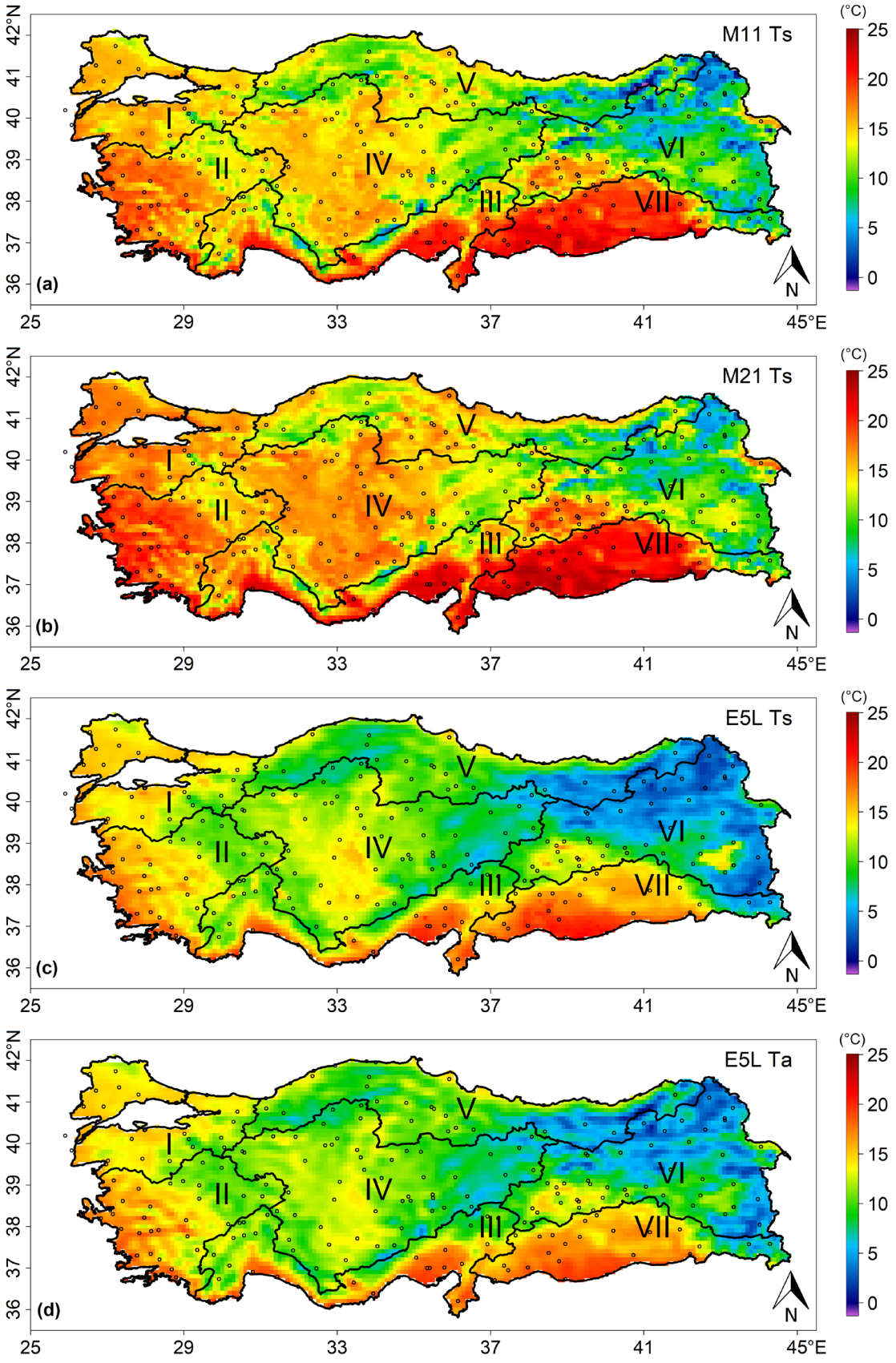

Fig. 2 Long term averages of the monthly: (a) M11 Ts, (b) M21 Ts, (c) E5L Ts, and (d) E5L Ta temperature products over the study area. Roman numbers I to VII indicate the seven geographical regions of Turkey: I – Marmara (MAR), II – Aegean (AEG), III –

Mediterranean (MED), IV - Central Anatolia (CE-ANA), V – Black Sea (BL-SEA), VI – Eastern Anatolia (EA-ANA), and VII – Southeastern Anatolia (SE-ANA). Black dots indicate the meteorological stations (total 266) where observations are taken.

Figs. 2 and 3 illustrate the monthly and regional variability of point-based temperatures, whereas Fig. 5 shows the temporal variability of average point-based temperature products. For STA Ta, M11 Ts, M21 Ts, E5L Ts, and E5L Ta, the average temperatures in 2000-2021 are 13.74, 15.32, 16.81, 12.51, and 12.74 °C, respectively. Overall, MODIS estimates (M11 Ts and M21 Ts) are on average 2.33 °C warmer than STA Ta, while ERA5-Land estimates (E5L Ts and E5L Ta) are 1.12 °C colder than STA Ta (Yilmaz 2023). Map-based estimations and point estimates both demonstrate that MODIS products are approximately 3.3 °C warmer than ERA5-Land products, and that this difference is persistent over both time (Figs. 2 and 4) and space (Fig. 4). The distribution of average temperature estimates of M21 Ts is similar to STA Ta (i.e., the width and median value of green and yellow boxes are similar) during colder months (November-February), however the median of M21 Ts is considerably higher than STA Ta during warmer months (Fig. 3). The behavior of ERA5-Land products is comparable, but the difference from STA Ta is less. In the summer (JJA) and winter (DJF), E5L Ts is typically 1.5 °C warmer and 1.9 °C colder than E5L Ta. On the other hand, M21 Ts is 5.5 °C warmer and 0.5 °C colder than STA Ta during summer and winter months, respectively.

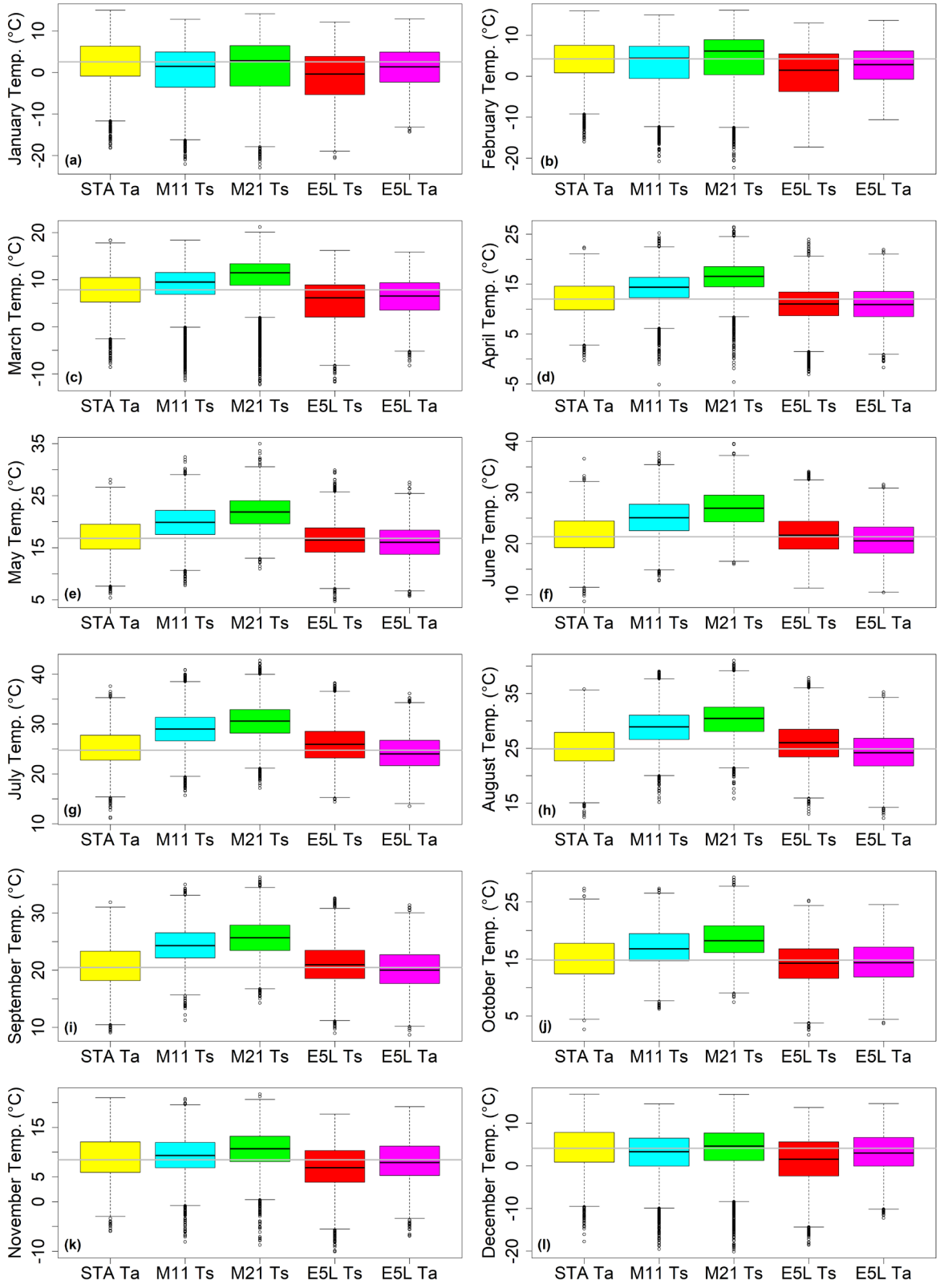

Fig. 3 Temporal variability of boxplot distributions of point-based average temperatures obtained over 266 stations from STA Ta, M11 Ts, M21 Ts, E5L Ts, and E5L Ta for 12 months: (a) January – (l) December

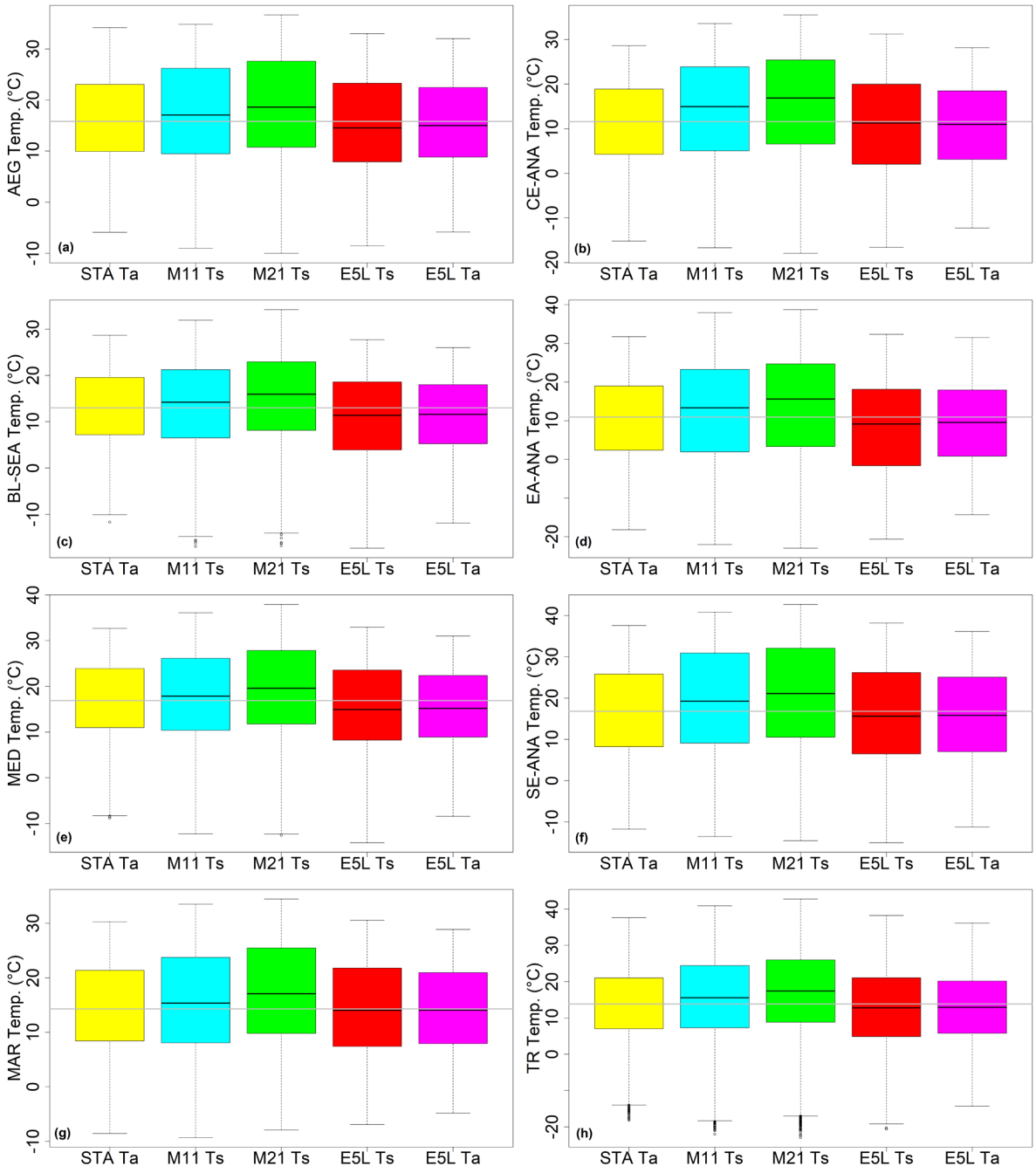

Fig. 4 Spatial variability of boxplot distributions of point-based average temperatures obtained over 266 stations from STA Ta, M11 Ts, M21 Ts, E5L Ts, and E5L Ta for seven geographical regions: (a) AEG, (b) CE-ANA, (c) BL-SEA, (d) EA-ANA, (e) MED, (f) SE-ANA, (g) MAR, and for Turkey: (h) TR

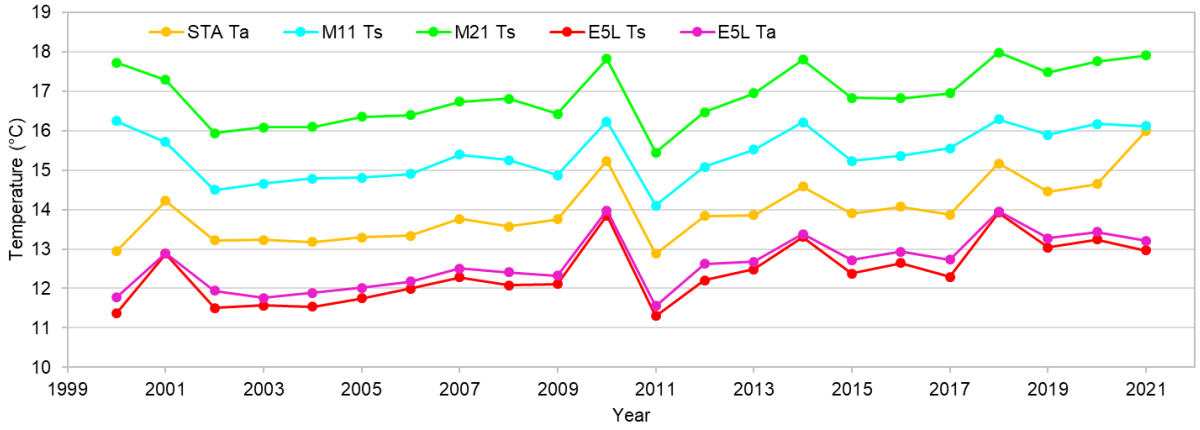

Fig. 5 Time series of the point-based annual mean temperatures obtained over 266 stations from STA Ta, M11 Ts, M21 Ts, E5L Ts, and E5L Ta

Fig. 6 and Table 3 both demonstrate the spatial distribution of the products' standard deviation. Overall, the coastal regions have less seasonal temperature variability than the inlands, where the snow-dominated EA-ANA region having the most seasonal variability among all regions. Compared to ERA5-Land products, the disparity between the regions is more apparent with MODIS. In general, MODIS products outperform ERA5-Land products in terms of their sensitivity to the transition between coastal and continental regions. While there isn't much of a difference in the transition sensitivity of M11 Ts and M21 Ts, there is higher difference between E5L Ts and E5L Ta (Fig. 6). In general, the standard deviation is smaller in the warmest six months (May to October) than the coldest six months (November to April), with February having nearly twice the standard deviation of the warmer months (Table 4).

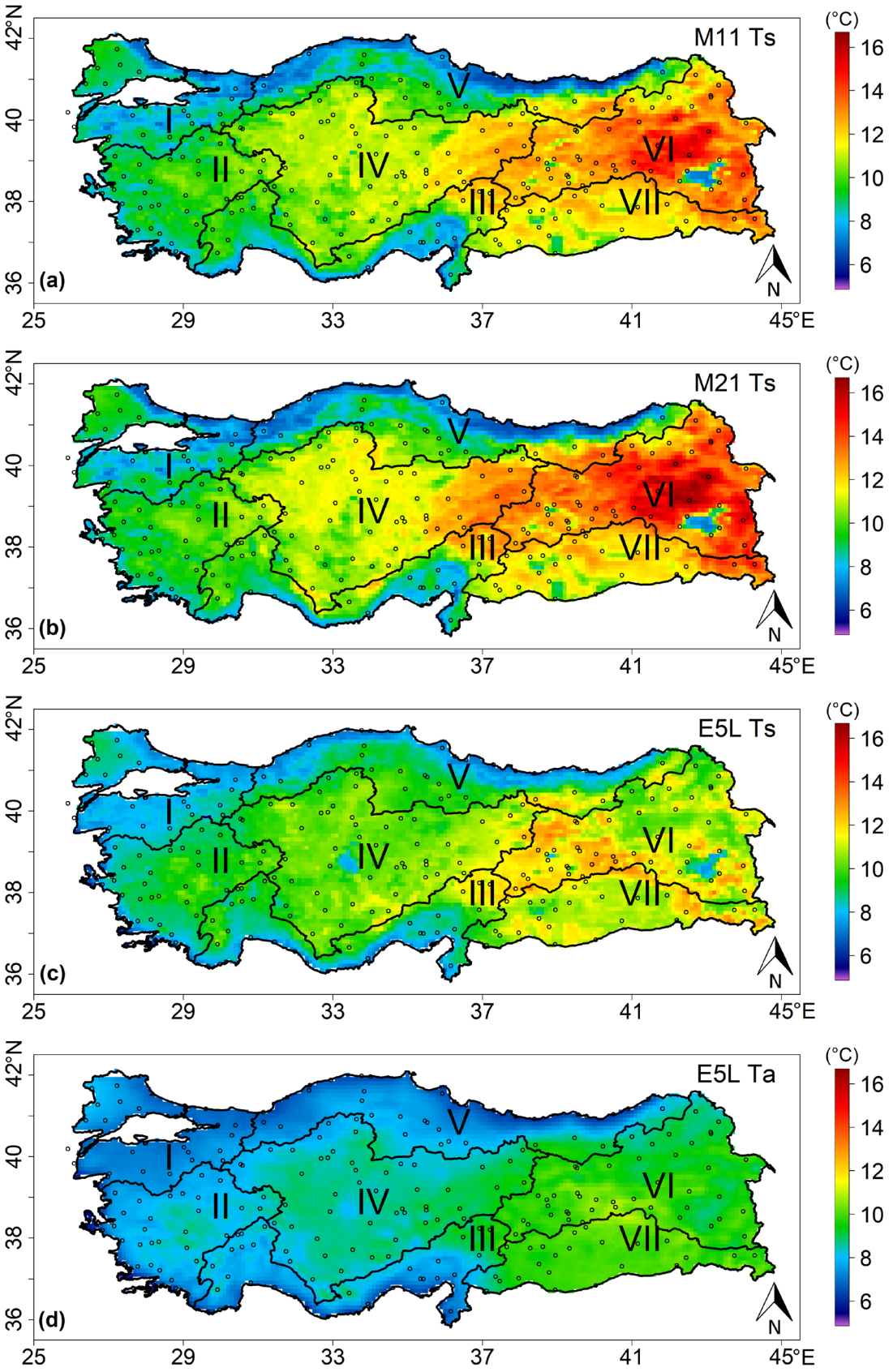

Fig. 6 Standard deviations of the monthly: (a) M11 Ts, (b) M21 Ts, (c) E5L Ts, and (d) E5L Ta temperature products over the study area

Table 4 Temporal variability of map-based statistics of M11 Ts, M21 Ts, E5L Ts, and E5L Ta products over the study area (TR) and seven geographical regions of Turkey

Map-based Statistics	Products	Months											
		Jan	Feb	Mar	Apr	May	Jun	Jul	Aug	Sep	Oct	Nov	Dec
Mean (°C)	M11 Ts	-1.82	0.58	6.33	12.33	18.06	23.49	27.63	27.57	23.10	15.60	7.71	0.83
	M21 Ts	-1.08	1.56	7.96	14.60	20.32	25.37	29.23	29.08	24.46	17.13	9.06	1.83
	E5L Ts	-2.66	-0.87	3.85	9.36	15.15	20.43	24.72	24.80	19.76	12.89	5.34	-0.55
	E5L Ta	-0.63	0.88	4.65	9.36	14.49	19.18	22.79	22.90	18.68	12.90	6.44	1.27
Standard Deviation (°C)	M11 Ts	2.52	3.10	2.45	1.95	1.57	1.40	1.27	1.36	1.53	1.64	2.18	2.71
	M21 Ts	2.91	3.44	2.78	2.08	1.54	1.37	1.29	1.38	1.54	1.74	2.32	3.01
	E5L Ts	2.39	2.60	2.36	1.69	1.32	1.24	1.11	1.25	1.47	1.57	1.91	2.46
	E5L Ta	1.98	2.16	2.07	1.70	1.34	1.15	1.04	1.23	1.48	1.56	1.84	2.11
Anomaly Correlation	M11 Ts& M21 Ts	0.95	0.96	0.96	0.94	0.94	0.93	0.94	0.94	0.95	0.95	0.97	0.96
	M11 Ts& E5L Ts	0.81	0.85	0.83	0.80	0.74	0.76	0.80	0.83	0.87	0.81	0.89	0.84
	M11 Ts& E5L Ta	0.84	0.89	0.85	0.85	0.78	0.73	0.77	0.83	0.86	0.82	0.91	0.87
	M21 Ts& E5L Ts	0.79	0.84	0.82	0.78	0.72	0.77	0.81	0.84	0.87	0.82	0.88	0.82
	M21 Ts& E5L Ta	0.81	0.87	0.84	0.83	0.76	0.75	0.78	0.83	0.86	0.82	0.90	0.85
	E5L Ts& E5L Ta	0.96	0.96	0.97	0.96	0.95	0.96	0.95	0.98	0.98	0.98	0.97	0.97
Trend (°C/decade)	M11 Ts	0.24	2.15	0.68	0.83	0.37	-0.32	-0.26	0.34	0.51	0.44	0.86	1.40
	M21 Ts	0.23	2.26	0.73	0.76	0.47	-0.01	-0.07	0.55	0.58	0.41	0.90	1.55
	E5L Ts	0.75	1.46	0.79	0.53	0.91	0.34	0.24	0.46	0.92	0.67	0.98	1.10
	E5L Ta	0.72	1.34	0.58	0.57	0.98	0.42	0.27	0.51	0.89	0.73	0.87	1.06

3.2 Correlation of Temperature Products

Overall, the total variability of the products can be decomposed into seasonality and the remaining anomaly components. Similarly, correlation between two products (i.e., cross-correlation) can be determined separately for the total, seasonality, and anomaly components. Given that the study area's seasonal temperature pattern is well known—summers are significantly warmer than winters—it is more intriguing to investigate the correlations between the anomaly components (Fig. 7) rather than total products. Overall, same family correlations (i.e., between the two MODIS or two ERA5-Land products) are ~0.95 while MODIS vs ERA5-Land correlations are around ~0.82 (Table 3). On average, M11 & E5L

correlations are 0.01 higher than M21 & E5L, where the correlations between these two products are much lower over water bodies (0.60-0.85) than over land (~0.95) (Fig. 7, for instance over Lake Van with centroid coordinates 38.6°N and 42.9°E). Similarly, E5L Ta & MODIS correlations are 0.01 higher than those between E5L Ts & MODIS. Average seasonal correlations are 0.90, 0.88, 0.85, and 0.84 during autumn, winter, spring, and summer respectively, where November correlations are the highest (0.92) and May-June are the lowest (0.82) (Table 4). In general, correlations between MODIS and E5L Ts are significantly lower than those between MODIS and E5L Ta, particularly over colder areas in EA-ANA and warmer SE-ANA regions (Fig. 7 and Table 3), as well as during April (Table 4).

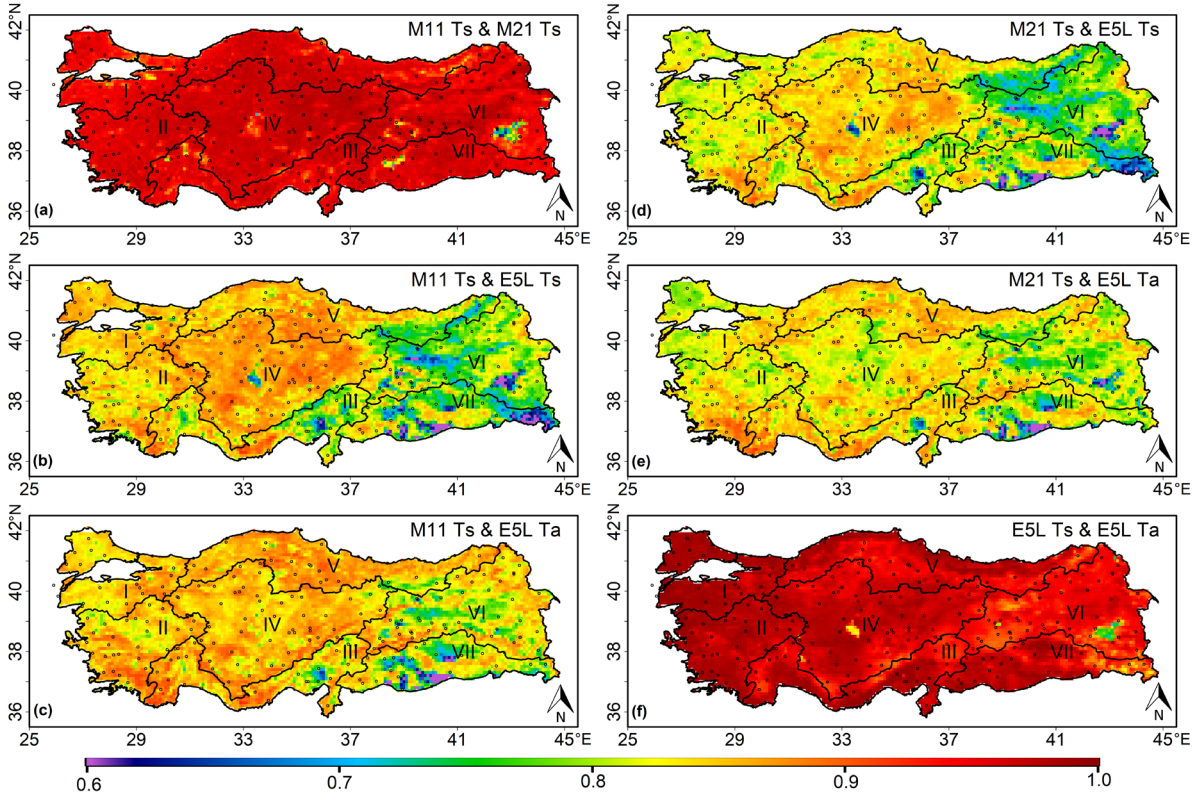

Fig. 7 Anomaly correlations between the map-based temperature product pairs: (a) M11 Ts & M21 Ts, (b) M11 Ts & E5L Ts, (c) M11 Ts & E5L Ta, (d) M21 Ts & E5L Ts, (e) M21 Ts & E5L Ta, and (f) E5L Ts & E5L Ta

3.3 Trends of Temperature Products

Spatial variability of temperature trends obtained utilizing map-based datasets are shown in Fig. 8 and Tables 3 and 4. With the exception of the MAR region, the spread of ERA5-Land trends is generally more comparable to station-based trends, where MODIS trends show more disparities with stations. In comparison to M11 Ts (0.66 °C/decade) and M21 Ts (0.74 °C/decade) trends, ERA5-Land trends significantly higher on average (0.94 °C/decade). Over the AEGEAN and SE-ANA regions, ERA5-Land products have much greater average trends (0.90 °C/decade) than MODIS products (0.48 °C/decade), whereas their average trends are the same over the EA-ANA region. The relative ranking of trends varies by month (Table 4); in instance, ERA5-Land trends during May, June, and July (0.53 °C/decade) are noticeably greater than MODIS trends (0.03 °C/decade). On the contrary, ERA5-Land trends during February (1.40 °C/decade) are much lower than MODIS (2.21 °C/decade) trends.

Temporal and regional variability of point-based trend estimates are shown in Figs. 8 and 9. These results show average STA Ta trends (0.98 °C/decade) are higher than those of M11 Ts and M21 Ts (0.65 and 0.73 °C/decade, respectively), and E5L Ts and E5L Ta (0.94 and 0.90 °C/decade, respectively) (Fig. 10). Average map-based trend estimates over entire Turkey (Table 3) also show similar trend magnitudes (0.66, 0.74, 0.96, and 0.92 °C/decade for M11 Ts, M21 Ts, E5L Ts, and E5L Ta, respectively). Accordingly, on average map- and point-based estimates are very consistent. For all regions, the tendency remains the same—STA Ta trends are larger than both MODIS and ERA5-Land trend estimates. Similarly,

ERA5-Land trends are consistently higher than MODIS trends (Fig. 10). Relative ranking of point-based monthly trends is consistent with this behavior, except for couple months: MODIS trends during February, April, and December are higher than both ground-observations and ERA5-Land (Fig. 9). In general, the trends for all products are higher in February and December than in any other month (Yilmaz 2023), and the trends for both MODIS products are highest in February (2.0 °C/decade) and lowest in June (- 0.07 °C/decade), respectively (Fig. 9). The STA Ta, M11 Ts, M21 Ts, E5L Ts, and E5L Ta trends in Fig. 9 have average interquartile ranges (IQR) of 0.47, 0.60, 0.73, 0.45, and 0.38 °C/decade, respectively. For the trends presented in Fig. 10, the average IQR for STA Ta, M11 Ts, M21 Ts, E5L Ts, and E5L Ta are 0.237, 0.239, 0.322, 0.188, and 0.158 °C/decade, respectively. As a result, MODIS products have greater IQR than station and ERA5-Land products (particularly in February, CE-ANA, and EA-ANA), and IQR for all products is also higher in February and over EA-ANA than other months and regions, respectively. On the other hand, IQR for MAR and August-November is typically lower than other regions and months (Figs. 8 and 9), in particular for ERA5-Land products across the MAR region (Fig. 10). Overall, compared to other regions, the EA-ANA region has the highest trends (>1.0 °C/decade) for all products.

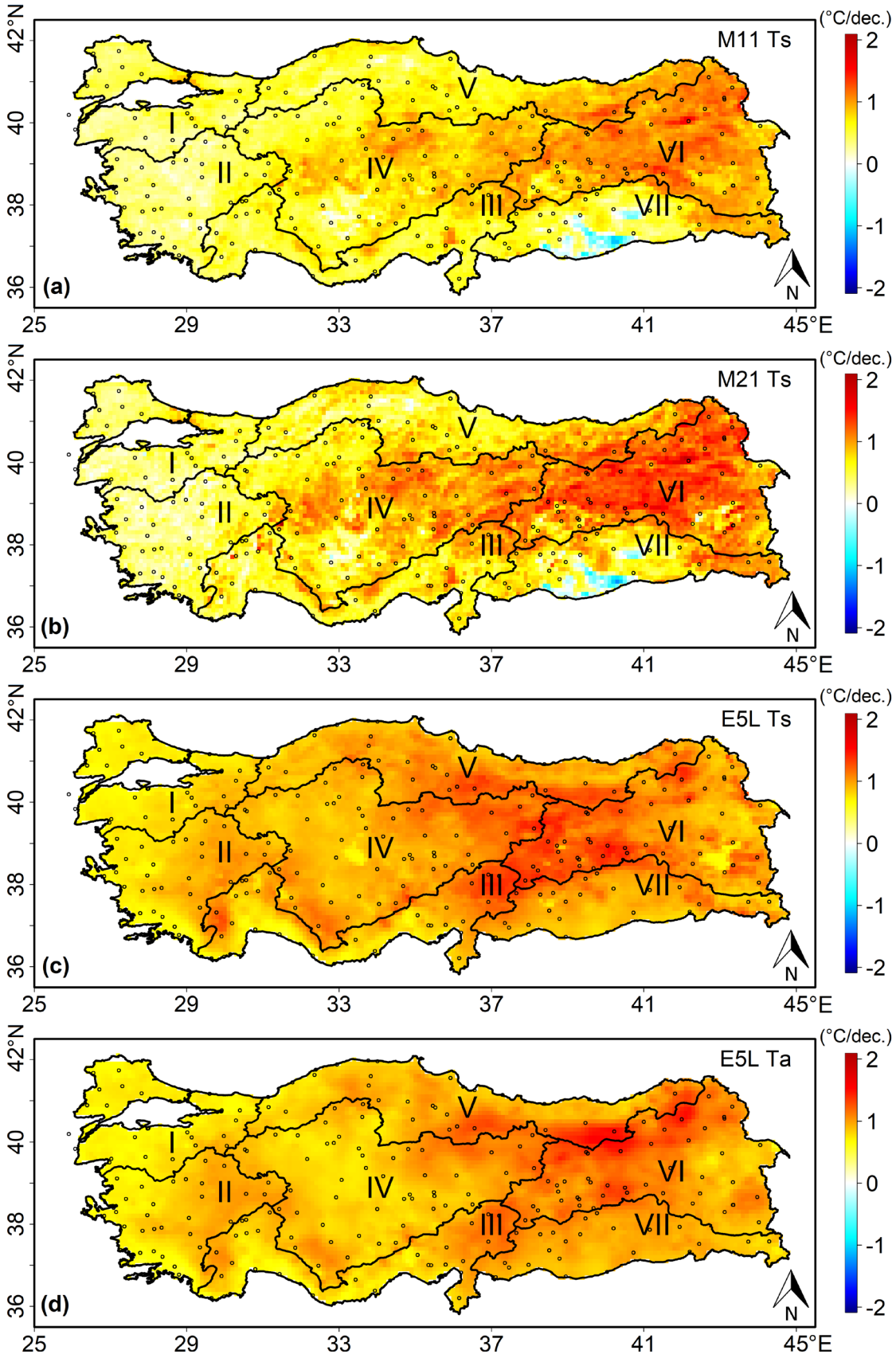

Fig. 8 Trends of the monthly: (a) M11 Ts, (b) M21 Ts, (c) E5L Ts, and (d) E5L Ta temperature products over the study area

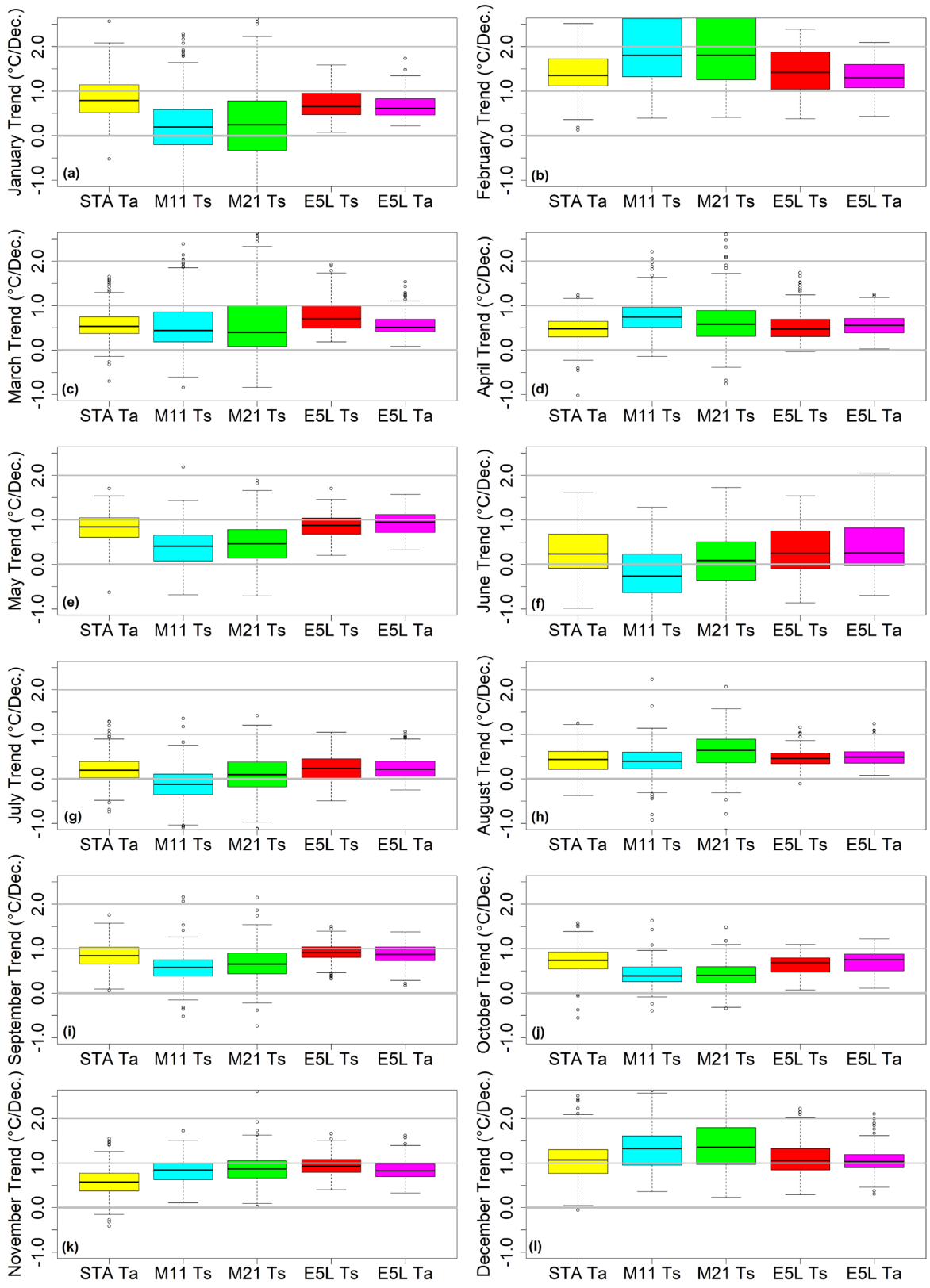

Fig. 9 Temporal variability of boxplot distributions of point-based temperature trends obtained over 266 stations from STA Ta, M11 Ts, M21 Ts, E5L Ts, and E5L Ta for 12 months: (a) January – (l) December

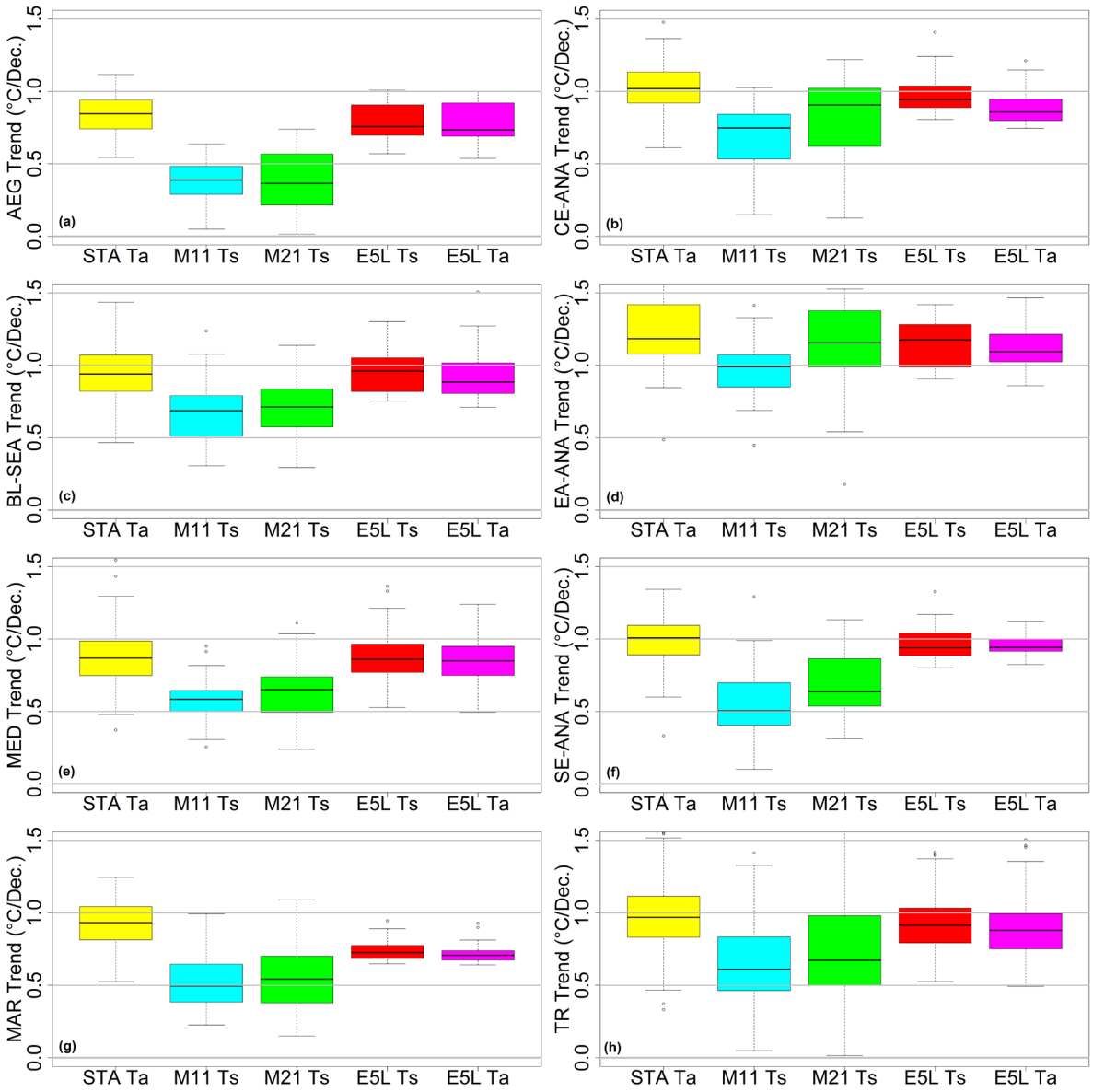

Fig. 10 Spatial variability of boxplot distributions of point-based temperature trends obtained over 266 stations from STA Ta, M11 Ts, M21 Ts, E5L Ts, and E5L Ta for seven geographical re-gions: (a) AEG, (b) CE-ANA, (c) BL-SEA, (d) EA-ANA, (e) MED, (f) SE-ANA, (g) MAR, and for Turkey: (h) TR

3.4 Statistics of Temperature Differences

Spatial distribution of the mean, standard deviation, and trend of the difference between the products (i.e., the total six combinations for the four products) are shown in Figs. 10-12, while Tables 4 and 5 present their average statistics. For all products, the average absolute temperature difference over Turkey is 2.4 °C (Fig. 11 and Table 5). The magnitude

of the temperature differences varies in space and time. Analysis of regional distributions reveals that, on average, the CE-ANA and SE-ANA regions have the biggest absolute difference (2.8 °C) and the MAR region has the lowest (1.6 °C) across the four products (Table 5). In comparison to other seasons and regions, the largest differences between M21 Ts and E5L Ta occur during summer (6.3 °C) and over SE-ANA (4.8 °C). On the other hand, the average difference during the coldest months (November – March) are highest for the difference between M21 Ts and E5L Ts products (Table 6). While the absolute differences between the products during the colder months are smaller than those during the warmer months (1.1 °C for January and 3.7 °C for July), analyses of the seasonality of the temperature differences demonstrate that this pattern persistently depends on temperature rates (Table 6).

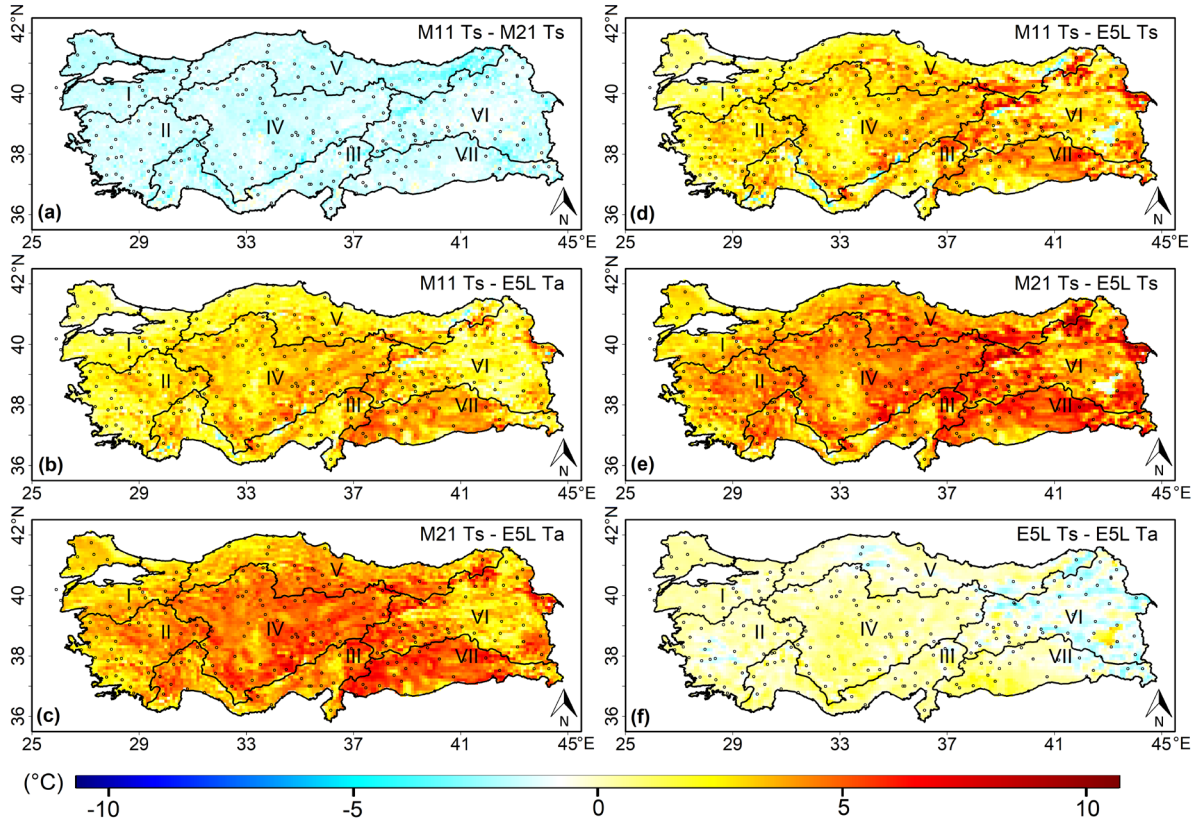

Fig. 11 Long term average of the map-based temperature differences between the products pairs: (a) M11 Ts – M21 Ts, (b) M11 Ts – E5L Ts, (c) M11 Ts – E5L Ta, (d) M21 Ts – E5L Ts, (e) M21 Ts – E5L Ta, and (f) E5L Ts – E5L Ta

The EA-ANA region, which is cold and snow-dominant, has the highest standard deviation of temperature differences (2.93 °C), whereas coastal and warmer regions (MAR, AEG, and MED) have significantly lower standard deviations (1.43 °C). The average standard deviation of all temperature differences is 1.94 °C (Fig. 12 and Table 5). When the temperature differences for each month are taken into account separately, the two MODIS products have an average standard deviation of the difference (0.63 °C) that is higher than the two ERA5-Land products (0.48 °C). However, when the entire year datasets are taken into account, the relative rankings are reversed (0.91 and 1.53 °C for MODIS and ERA5-Land products, respectively). The trends of the differences between the MODIS and ERA5-Land estimates are particularly more pronounced over the warmer SE-ANA and the coastal regions as opposed to interior and colder regions (Fig. 13). While generally the trend of temperature difference between MODIS and ERA5-Land is positive over the coldest EA-ANA, it is negative over all of the four coastal regions. Similar to this, E5L Ts generally has a higher temperature difference trend than E5L Ta, with the exception of the EA-ANA region.

Table 5 Spatial variability of map-based statistics of temperature differences between M11 Ts, M21 Ts, E5L Ts, and E5L Ta products over the study area (TR) and seven geographical regions of Turkey

Difference Statistics	Product Differences	Regions							
		TR	MAR	AEG	MED	CE-ANA	BL-SEA	EA-ANA	SE-ANA
Mean (°C)	M11 Ts–M21 Ts	-1.51	-1.63	-1.42	-1.49	-1.51	-1.67	-1.45	-1.41
	M11 Ts–E5L Ts	2.44	1.08	2.14	1.98	2.71	2.36	2.83	3.27
	M11 Ts–E5L Ta	2.39	1.25	2.14	2.29	3.04	2.02	2.09	3.37
	M21 Ts–E5L Ts	3.95	2.71	3.56	3.47	4.22	4.03	4.28	4.68
	M21 Ts–E5L Ta	3.90	2.88	3.56	3.78	4.55	3.69	3.54	4.77
	E5L Ts–E5L Ta	-0.05	0.17	0.00	0.31	0.33	-0.34	-0.75	0.10
Standard Deviation (°C)	M11 Ts–M21 Ts	0.91	0.67	0.67	0.81	0.97	0.81	1.31	0.75
	M11 Ts–E5L Ts	1.72	1.24	1.28	1.32	1.66	1.56	2.70	1.68
	M11 Ts–E5L Ta	2.49	1.62	1.88	1.94	2.80	1.96	3.77	2.36
	M21 Ts–E5L Ts	2.09	1.44	1.54	1.56	2.15	1.79	3.40	1.84
	M21 Ts–E5L Ta	2.91	1.83	2.17	2.32	3.29	2.19	4.55	2.56
	E5L Ts–E5L Ta	1.53	0.90	1.17	1.44	1.80	1.49	1.87	1.37
Trend (°C/decade)	M11 Ts–M21 Ts	-0.08	0.02	-0.02	-0.08	-0.12	-0.04	-0.15	-0.13
	M11 Ts–E5L Ts	-0.13	-0.18	-0.31	-0.18	-0.07	-0.16	0.09	-0.31
	M11 Ts–E5L Ta	-0.11	-0.17	-0.31	-0.15	-0.02	-0.15	0.08	-0.31
	M21 Ts–E5L Ts	-0.04	-0.20	-0.29	-0.10	0.04	-0.12	0.24	-0.18
	M21 Ts–E5L Ta	-0.03	-0.19	-0.29	-0.06	0.10	-0.12	0.22	-0.17
	E5L Ts–E5L Ta	0.04	0.20	0.29	0.10	-0.04	0.12	-0.24	0.18

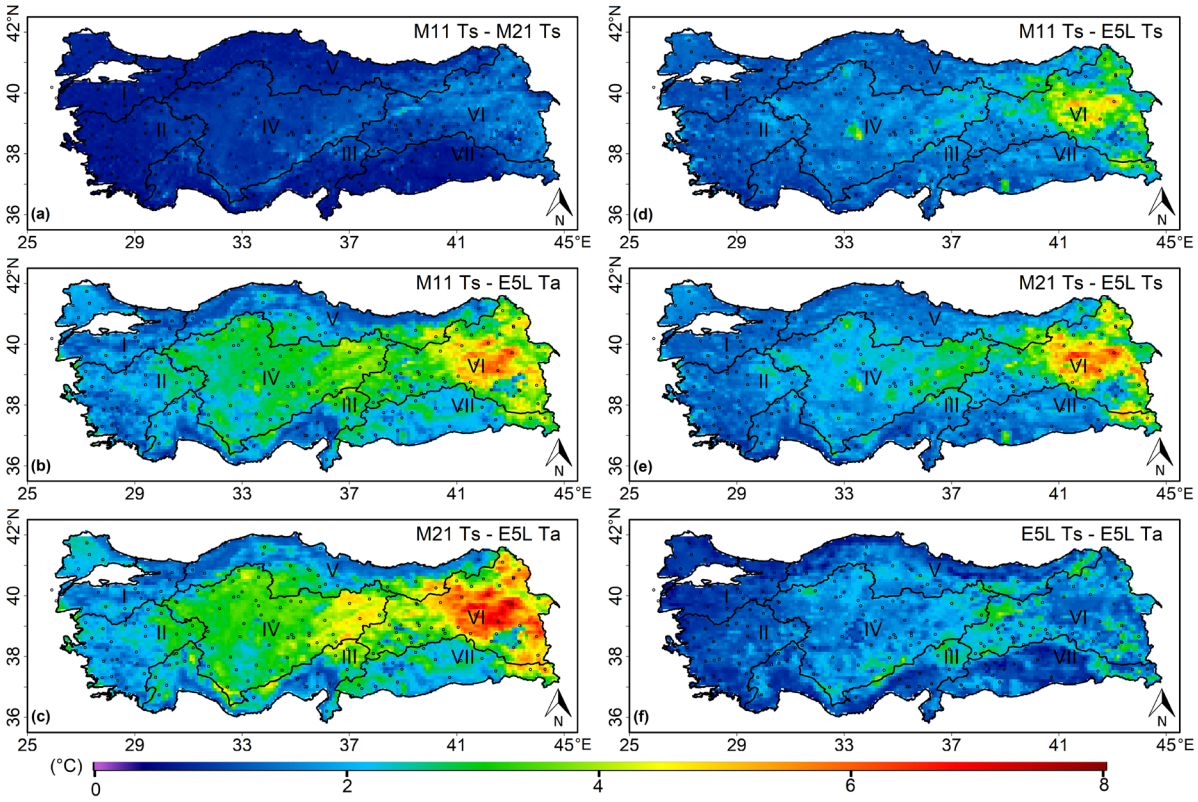

Fig. 12 Standard deviations of the map-based temperature differences between the products

pairs: (a) M11 Ts – M21 Ts, (b) M11 Ts – E5L Ts, (c) M11 Ts – E5L Ta, (d) M21 Ts – E5L Ts, (e) M21 Ts – E5L Ta, and (f) E5L Ts – E5L Ta

Table 6 Temporal variability of map-based statistics of temperature differences between M11 Ts, M21 Ts, E5L Ts, and E5L Ta products over the study area (TR) and seven geographical regions of Turkey

Difference Statistics	Product Differences	Months											
		Jan	Feb	Mar	Apr	May	Jun	Jul	Aug	Sep	Oct	Nov	Dec
Mean (°C)	M11 Ts–M21 Ts	-0.74	-0.98	-1.63	-2.27	-2.25	-1.88	-1.60	-1.51	-1.36	-1.53	-1.35	-1.00
	M11 Ts–E5L Ts	0.84	1.45	2.49	2.97	2.91	3.06	2.91	2.77	3.34	2.71	2.37	1.38
	M11 Ts–E5L Ta	-1.20	-0.30	1.69	2.97	3.57	4.32	4.83	4.67	4.42	2.70	1.27	-0.44
	M21 Ts–E5L Ts	1.58	2.43	4.12	5.25	5.17	4.94	4.52	4.28	4.70	4.24	3.72	2.38
	M21 Ts–E5L Ta	-0.46	0.68	3.32	5.24	5.82	6.19	6.44	6.18	5.78	4.23	2.62	0.56
	E5L Ts–E5L Ta	-2.04	-1.75	-0.80	0.00	0.66	1.26	1.92	1.90	1.08	-0.01	-1.10	-1.82
Standard Deviation (°C)	M11 Ts–M21 Ts	0.87	0.89	0.77	0.73	0.51	0.47	0.42	0.43	0.45	0.54	0.59	0.85
	M11 Ts–E5L Ts	1.49	1.65	1.46	1.25	1.08	0.90	0.77	0.72	0.76	0.95	1.04	1.50
	M11 Ts–E5L Ta	1.41	1.59	1.36	1.08	0.98	0.96	0.82	0.76	0.79	0.94	0.93	1.40
	M21 Ts–E5L Ts	1.82	1.93	1.67	1.41	1.09	0.87	0.77	0.73	0.77	0.96	1.13	1.76
	M21 Ts–E5L Ta	1.79	1.94	1.62	1.24	1.02	0.91	0.82	0.76	0.82	0.97	1.08	1.69
	E5L Ts–E5L Ta	0.71	0.77	0.61	0.52	0.39	0.36	0.37	0.28	0.27	0.29	0.45	0.70
Trend (°C/decade)	M11 Ts–M21 Ts	0.01	-0.12	-0.05	0.07	-0.09	-0.30	-0.19	-0.21	-0.07	0.03	-0.04	-0.15
	M11 Ts–E5L Ts	-0.14	0.70	-0.11	0.30	-0.54	-0.66	-0.50	-0.12	-0.41	-0.23	-0.12	0.31
	M11 Ts–E5L Ta	-0.14	0.81	0.10	0.26	-0.61	-0.74	-0.53	-0.17	-0.38	-0.30	-0.01	0.34
	M21 Ts–E5L Ts	-0.15	0.81	-0.05	0.23	-0.45	-0.36	-0.31	0.09	-0.34	-0.26	-0.08	0.45
	M21 Ts–E5L Ta	-0.14	0.93	0.15	0.19	-0.51	-0.43	-0.34	0.04	-0.31	-0.33	0.04	0.49
	E5L Ts–E5L Ta	0.15	-0.81	0.05	-0.23	0.45	0.36	0.31	-0.09	0.34	0.26	0.08	-0.45

4 Discussion

4.1 Ts vs Ta – Long-term Averages

The nature of the temperature values compared in this study differs (Ts vs Ta). Warmer medium would radiate toward colder medium among two very close mediums, reaching balance over long periods of time—like 22 years—and large regions—like Turkey's surface area, ~784,000 km^2. Overall, when average values are taken over long term and large regions, the mean differences, particularly between the trends, are expected to disappear: on average there is no reason for long term and large region averaged Ts to deviate from Ta (i.e.,

due to lapse rate, which is not directly related to trend changes, the temperature difference between two places with a 2m elevation difference is expected to be only 0.02 °C). Accordingly, persistent patterns may exist at monthly or seasonal timeframes, but it is anticipated that long-term and large-region averages of these products' tendencies will converge. The behavior is supported by the map-based ERA5-Land model results, which show that the difference between the long-term averages of E5L Ts and E5L Ta is only 0.05 °C (Table 5 and Fig. 5). The results that the bias between the Ts and Ta estimates of ERA5-Land over the long term is only marginal are also supported by the temperature differences between these two ERA5-Land products over ground station locations, where the average temperatures for E5L Ts and E5L Ta are 12.51 and 12.74 °C, respectively. While the differences between E5L Ts and E5L Ta estimates are almost negligible, those between the same-type M11 Ts and M21 Ts are not; both map- (Tables 5 and 6) and point-based (Table 7 and Fig. 5) analyses suggest that M21 Ts is, on average, 1.5 °C warmer than M11 Ts. The long-term biases between different product families, however, are greater than the biases between different variables for the same family—point-based MODIS, ERA5-Land, and station mean temperatures are 16.07, 13.74, and 12.62 °C, respectively (Table 7). Here, average station-based temperature observations are in between MODIS and ERA5-Land temperatures but not any closer to E5L Ta estimates than MODIS and/or E5L Ts (Fig. 5).

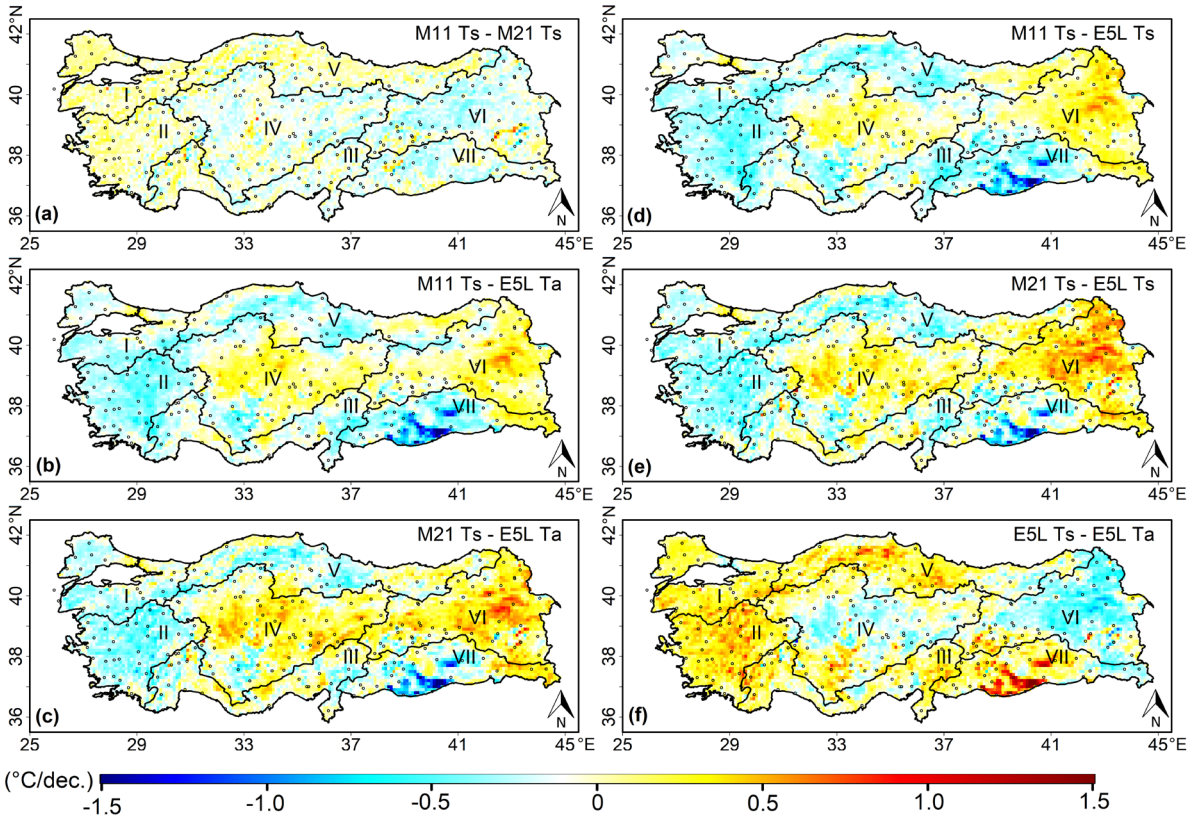

Fig. 13 Trends of the map-based temperature differences between the products pairs: (a) M11 Ts – M21 Ts, (b) M11 Ts – E5L Ts, (c) M11 Ts – E5L Ta, (d) M21 Ts – E5L Ts, (e) M21 Ts – E5L Ta, and (f) E5L Ts – E5L Ta

Table 7 Spatial variability of point-based statistics of M11 Ts, M21 Ts, E5L Ts, and E5L Ta products over entire study area (TR) and seven geographical regions of Turkey

Point-based Statistics	Products	Regions							
		TR	MAR	AEG	MED	CE-ANA	BL-SEA	EA-ANA	SE-ANA
Mean (°C)	STA Ta	13.74	14.6	16.2	16.8	11.4	13.0	10.6	16.8
	M11 Ts	15.32	15.6	17.5	17.7	14.1	13.5	12.3	19.3
	M21 Ts	16.81	17.4	18.9	19.3	15.5	15.2	13.6	20.7
	E5L Ts	12.51	14.4	15.1	15.1	10.9	10.7	8.5	16.0
	E5L Ta	12.74	14.2	15.4	15.1	10.8	11.2	9.6	15.8
Trend (°C/decade)	STA Ta	0.99	0.90	0.83	0.92	1.02	0.95	1.22	0.98
	M11 Ts	0.65	0.54	0.38	0.57	0.69	0.66	0.98	0.56
	M21 Ts	0.73	0.57	0.38	0.65	0.83	0.69	1.11	0.71
	E5L Ts	0.94	0.74	0.79	0.89	0.97	0.98	1.15	0.97
	E5L Ta	0.90	0.72	0.78	0.85	0.88	0.93	1.11	0.96

549 **4.2 Ts vs Ta – Bias Seasonality**

550 Products from MODIS are consistently warmer than those from ERA5-Land (Table
551 6). Systematic strong seasonality can be expected between the difference between Ts and Ta
552 estimations of these two products, much like the temperature signal that exhibits strong
553 seasonality. Due to their random retrieval errors and the different nature of the two products
554 (i.e., Ts vs Ta), MODIS-based Ts estimations and STA Ta differ from one another. Since
555 there are both Ts and Ta simulations, it is possible to use ERA5-Land estimations to
556 decompose the existing difference between MODIS Ts and STA Ta products into these two
557 components. Above results and discussions show while there are systematic differences
558 between MODIS Ts and E5L Ta, the nature of the retrieval algorithms—rather than the
559 estimates themselves—is primarily responsible for these differences in long-term and large
560 region averages. Ts estimations are typically 1.70 °C warmer than Ta during the summer and
561 1.87 °C colder during the winter, according to map-based ERA5-Land products. As a result, it
562 may be inferred that for the identical retrieval platform over the study domain, there exists an
563 average 1.79 °C systematic difference between Ts and Ta estimations during summer (i.e., Ts
564 - Ta = 1.79 °C) and winter (i.e., Ta - Ts = 1.79 °C). Point-based analyses reveal that M21 and
565 M11 Ts products, on average, have a summer warm bias of 5.40 and 3.80 °C, respectively,
566 compared to STA Ta, while the winter warm biases are -0.46 and -1.50 °C, respectively
567 (Table 8). When the 1.79 °C bias (i.e., Ts against Ta) is eliminated from these MODIS
568 estimations, the temperature bias of the M21 and M11 Ts products becomes 3.61 and 2.01 °C,
569 respectively, during summer and 1.33 and 0.29 °C, during winter (i.e., compared against

570 "non-existent but expected" Ts observations). Although the 1.79 °C bias estimate obtained
571 from the ERA5-Land estimates heavily influences these results, they still demonstrate that the
572 M21 and M11 Ts products have bias that is dependent on temperature rate, with warmer
573 summer temperatures being linked to higher warm bias rates than colder winter months.
574
575 **Table 8** Temporal variability of point-based statistics of M11 Ts, M21 Ts, E5L Ts, and E5L
576 Ta products over entire study area (TR) and seven geographical regions of Turkey

Point-based Statistics	Products	Months											
		Jan	Feb	Mar	Apr	May	Jun	Jul	Aug	Sep	Oct	Nov	Dec
Mean (°C)	STA Ta	2.4	3.9	7.7	12.1	17.0	21.6	25.1	25.1	20.8	15.1	8.9	4.1
	M11 Ts	0.3	2.9	8.6	14.1	19.8	25.2	29.1	28.9	24.4	17.1	9.3	2.7
	M21 Ts	1.2	4.0	10.3	16.3	21.8	27.0	30.6	30.4	25.8	18.5	10.6	3.8
	E5L Ts	-0.9	0.7	5.3	10.7	16.4	21.7	25.9	25.9	21.0	14.2	6.8	1.2
	E5L Ta	1.2	2.6	6.3	10.9	16.0	20.7	24.2	24.3	20.2	14.5	8.1	3.0
Trend (°C/decade)	STA Ta	0.86	1.44	0.59	0.47	0.81	0.28	0.19	0.41	0.84	0.74	0.58	1.09
	M11 Ts	0.29	2.02	0.59	0.77	0.37	-0.26	-0.14	0.41	0.60	0.42	0.82	1.36
	M21 Ts	0.28	2.11	0.64	0.66	0.48	0.06	0.05	0.63	0.67	0.41	0.88	1.48
	E5L Ts	0.72	1.45	0.78	0.53	0.86	0.30	0.23	0.46	0.92	0.65	0.95	1.10
	E5L Ta	0.68	1.32	0.57	0.57	0.93	0.38	0.25	0.50	0.88	0.70	0.85	1.05

577

578 **4.3 Standard Deviations and Anomaly Correlations**

579 When the average standard deviation of the differences between any two products are
580 taken into account (Table 5), E5L Ta (2.31 °C), M21 Ts (1.97 °C), E5L Ts (1.78 °C), and
581 M11 Ts (1.71 °C) are ranked highest to lowest. Investigating the relationships between the
582 anomaly components of these products would be important if it were assumed that these
583 standard deviations were caused by the random components of their errors and the variations
584 in the nature of these products. Overall, ERA5 outputs are less variable than MODIS, and
585 coastal regions (MAR, AEG, MED, BL-SEA) exhibit less variability than inlands with
586 terrestrial climate (CE-ANA, EA-ANA, and SE-ANA). The heat capacity difference between

the ocean and the atmosphere/land contributes significantly to this disparity. The sea warms and cools more slowly than land because water can store more heat. As a result, relative to inland areas, temperature variation is less in coastal locations. Compared to sea temperatures, land temperatures fluctuate rapidly. Inland regions experience greater temperature extremes because land absorbs and releases heat energy more quickly than water does. Abbasnia and Toros (2020) have investigated the variability of the trends in weather extremes including temperature and diurnal temperature range over coastal and inland regions of Turkey. They also concluded that in coastal zones, heat capacity of water tends to keep temperatures relatively stable in daily basis. This could imply the relative stability of monthly mean temperatures in coastal zones. As a result, analogous with the results of this research (Fig. 7 and Table 3), coastal regions have consistently experienced less variability than terrestrial locations.

Average anomaly correlation for the products mentioned above is 0.87 (Table 3) and total correlation is 0.98 (result not shown). Although their nature and retrieval algorithms are considerably different from one another, the anomaly correlations in this case are considered to be high enough to support the conclusion that the products reflect a similar signal. Similarly, the spatial correlation of average temperatures shown in Fig. 2 ranges between 0.965 and 0.995, implying that despite constant discrepancies in their mean values, the products reflect the spatial distribution's variability well. This suggests that, should estimation of one of the products utilizing others be relevant, post-processing algorithms (e.g. least squares- or machine learning-based) might better reduce these systematic differences.

4.4 Trend of Differences between Products

As shown in Table 4, map-based trends during February for MODIS (2.21 °C/decade) are significantly higher than those for ERA5-Land (1.40 °C/decade). This result is contrary to long-term map-based (MODIS and ERA5-Land trends are 0.70 and 0.94 °C/decade, respectively) and point-based (MODIS, ERA5-Land, and STA trends are 0.69, 0.92, and 0.99 °C/decade, respectively) that show MODIS has lower trends than both ERA5-Land and STA. MODIS warming trends during February are also significantly higher than the rates provided by (Yilmaz 2023) and an average climate change hot spot Mediterranean Basin. On the other hand, the sign of the trend of difference MODIS and ERA5-Land reverses during May and June (Table 6), where MODIS has an average trend of 0.54 °C/decade less than ERA5-Land. The reason for the higher temperature trends in the ERA5-Land- than MODIS-based temperatures could be attributed to several factors. These may include differences in the methodologies and assumptions used in the two datasets, variations in data processing techniques, or potential biases in either dataset. These varying results highlight the importance of examining the trend of differences between observation-, satellite-, and model-based estimates, where further analysis would be required to pinpoint the specific reasons for the discrepancy.

The overall trend of the differences between MODIS and ERA5-Land is strongly negative and distinct across the irrigated SE-ANA region when compared to other areas (Table 5 and Fig. 11). This result would be expected if the land cover map of the land surface model did not include irrigated regions, while satellite-based estimations, which make

far less assumptions about the ground condition. Although adding irrigation maps would be effortless, providing the land surface model of NWP models (such as ERA5-Land) with information regarding the amount of irrigated water may not always be simple. As a consequence, in irrigated areas, remote sensing-based products (like MODIS) have a distinct advantage in sensing the actual conditions, particularly for the estimation of variables that are related to the components of the water and/or energy balance (e.g, soil moisture and temperature).

The products investigated in this study have different nature; station-based observations and E5L Ta represent 2m air temperature, while MODIS and E5L Ts products indicate SKT/LST. However, the disparities between the Ts and Ta products of ERA5-Land's large region and long-term averages remain very small, whereas those across different product families (MODIS and ERA5-Land, or MODIS and observations) are more pronounced. There is no reason to predict higher or lower Ta than Ts over such long time scales and broad areas (here, datasets spanning 22 years are examined over entire Turkey). Instead, trends and averages of Ta and Ts temperatures could be expected to converge. As a result, rather than the nature of different variables—Ta vs Ts—, it is expected that disparities between different products are primarily caused by the estimation algorithms (e.g., MODIS vs ERA5-Land).

4.5 Topographical Complexity

The study area is considered to be very complex owing to its rapidly changing topography. In light of this, Table 9 investigates the variability of average temperature trends over Turkey in relation to changing slope characteristics. On average, the variability of the

trends and their errors are higher between the products (i.e., MxD and E5L) compared to those between the slope zones (i.e., 0 – 5%, 5 – 23.39%, where the highest slope in the area is 23.39%). In this study, S > 5% are regarded as complex, and slopes S < 5% are deemed non-complex (Amjad et al. 2020). MxD-based products have consistently lower trends than those of stations or E5L, while the errors of E5L-based products are significantly lower than those of MxD. Overall, for both products, complex regions (i.e., S > 5%) exhibit greater trends than non-complex regions (i.e., S < 5%). In comparison to MxD, where these statistics are lower over complex regions than non-complex, the standard deviation and the mean of the trend errors of E5L are generally smaller. These results imply overall E5L offers better temperature trend estimations than MxD both in terms of trend bias and error over both complex and non-complex regions.

Table 9 Variability of trends (°C/dec.) and trend errors (°C/dec.) with respect to terrain slope slope (S in %) and elevation (DEM in m).

Trend Statistics	S (%)	DEM (m)	STA (°C/dec.)	MxD (°C/dec.)	E5L (°C/dec.)	Err MxD (°C/dec.)	Err E5L (°C/dec.)	AbsErr MxD (°C/dec.)	AbsErr E5L (°C/dec.)
Mean (°C/dec.)	0 < S < 5	663	0.988	0.680	0.910	-0.312	-0.086	0.350	0.199
	5 < S < 23.39	807	0.958	0.721	0.942	-0.235	-0.019	0.295	0.167
	0 < S < 23.39	694	0.982	0.689	0.917	-0.296	-0.072	0.338	0.192
Standard Deviation (°C/dec.)	0 < S < 5	569	0.258	0.282	0.178	0.258	0.240	0.210	0.160
	5 < S < 23.39	590	0.190	0.311	0.195	0.273	0.204	0.210	0.115
	0 < S < 23.39	575	0.246	0.289	0.182	0.263	0.234	0.211	0.152

4.6 Station Density

In this study, a total of 266 stations were used spanning a 784.000 km^2 region, with one station being available on average over a 3000 km^2 area (Table 2). The World Meteorological

669 Organization (WMO 2008) provides recommendations for the minimum station densities (area
670 in km^2 per station). For accurate representation of precipitation over complex topography, an
671 observation station is advised for each 250 km^2 for non-recording sensors and 2500 km^2 for
672 recording sensors. A comparable estimate is not given for temperature, though. According to
673 Vose and Menne (2004), at least 25 stations are needed to identify temporal variability in the
674 spatial mean of temperature and precipitation, but this number rises to at least 135 for trend
675 detection. Although the research they conducted over the entire USA failed to define a specific
676 density requirement particularly over the complex topography, they came to the conclusion that
677 an increase in station number corresponded to improved performance indicators. This brings up
678 the issue of cost-benefit when constructing a dense network (Njoku et al. 2023).

679 While the average station density over the whole research area is roughly doubled in the
680 MAR, AEG, and SE-ANA regions (1700 km^2/station), the EA-ANA region has less than half
681 of this density (7200 km^2/station; Table 2). Given EA-ANA region is very mountainous and
682 have very complex topography, such a sparse station density is not considered sufficient for the
683 relevant region. Compared to recently installed automatic weather stations (AWOS)—
684 installation started in particular after 2010—which have a substantially greater station density
685 throughout the entire research region (300 km^2/station), these stations, which previously
686 gathered observations manually, had a rather low station density (3000 km^2/station). However,
687 the majority of these AWOS only collected data for a short period of time—many collected only
688 less than five years. The datasets derived from AWOS available in the region are not suitable

for performing the trend analysis done in this work considering the very high sampling errors of 5-year observational datasets.

For the entire study, especially across regions with relatively higher topographical complexity, manually observing station density is insufficient. This demonstrates the need of using model- or remote sensing-based datasets to provide representative estimates across the study area, and in particular across sub-regions. The accuracy analyses of the products are compared consistently in this study, and only datasets that are mutually available are used.

Considering gridded datasets provide an estimate for each 81 km^2 area (ERA5-Land spatial resolution), they are considered to exceed the spatial representation of stations (WMO 2008). This implies that representative regional trends can be estimated using these products rather than station-based observations due to the availability of gridded remote sensing- or model-based datasets spanning entire sub-regions.

The goal of this study is to intercompare the trends for various products at the same spatial resolution over the same grids, even though the available 3000 km^2/station density with non-recording gauges may not be adequate to acquire sufficiently low temperature representation errors in representing the entire study area. As a result, under the assumption that the performances remain relatively consistent in space, representation errors are not anticipated to have an impact on the findings of this study.

4.7 Temperature Under Changing Climate

Rising temperatures brought on by climate change are having globally significant impact. Between 2011 and 2020, the average global surface temperature was 1.09°C higher than it was between 1850 and 1900 (IPCC 2023). Overall, the warming over land during this time period (1.59°C) was higher than the warming over the ocean (0.88°C). Similarly, according to IPCC (2023), the average global surface temperature between 2001 and 2020 was 0.99 °C higher than it was between 1850 and 1900. This implies the years 2011 to 2020 will be on average 0.10 °C warmer than the years 2001 to 2020. Global average temperatures are 0.23 °C warmer between 2011 and 2020 than they were between 2001 and 2010 (NOAA). The region investigated in this study, which is situated in the Mediterranean basin, one of the hotspots for climate change (IPCC 2021b), is anticipated to experience warming conditions of up to 7.5 °C by the end of the century (Gumus et al. 2023). In the study region, the average station-based temperature for the period 2011–2020 is on average 0.45 °C warmer than for the period 2001–2010 (Figure 5). Given the global average estimates have much smaller sampling errors, the averages presented in this study have much higher sampling errors, for example, 2010 is a much warmer year and 2011is a much colder year relative to long term trends. The disparity between the two successive decades is lessened by these two single-year deviations from the trends. Here, the average temperature of 2012–2021 period is 0.99 °C higher than it was in 2000–2009, which is in line with the trends obtained in this study. As a result, the average warming over the study area (0.99 °C) is significantly higher than the global warming

rates (0.23 °C) mentioned above, highlighting the fact that the study area has already experienced greater adverse impacts from climate change than the global rates do.

5. Conclusions

In this study, the monthly temperature over Turkey between 2000 and 2021 was investigated using data from MODIS (M11 and M21 Ts), ERA5-Land (E5L Ts and E5L Ta), and ground station-based observations (STA Ta). The temporal and spatial variability of the trends and accuracy of these products were particularly examined and compared. Separate analyses were carried out for map- and point-based temperature estimates.

Overall E5L offers better temperature trend estimations than MxD both in terms of trend bias and error over both complex and non-complex regions. The average point-based temperatures from MODIS and ERA5-Land over stations are 1.7 °C warmer than the map-based averages calculated over the full study region, yet the bias of these products relative to one another (i.e., ranking of average temperature) remains quite comparable. When considering MODIS and ERA5-Land products, inter-family differences in the mean, the standard deviation, and the trend components are larger and more consistent than minor differences in the nature of products within the same family (such as between M11 and M21 Ts or between E5L Ts and E5L Ta). While M21 and M11 Ts products are 4.2 °C and 2.7 °C warmer than ERA5-Land products, respectively, point-based E5L Ts and E5L Ta products have similar means (12.6 °C). MODIS-based products also show larger monthly variability (standard deviation 10.6 °C) compared to ERA5-Land results (9.2 °C). On the other

hand, ERA5-Land has larger trends (0.94 °C) while MODIS products exhibit lesser trends (0.70 °C).

Despite the differences between the statistics of these estimates showing some variability in time and space, the ranking of these differences is systematic and consistent, with certain exceptions (for instance, MODIS trends during February are 2.2 °C/decade while ERA5-Land on average are 1.4 °C/decade). Such systematic discrepancies are largely eliminated using post-processing algorithms—linear regression or machine learning—, while such modified datasets are expected to exhibit consistent temporal and spatial variability.

For the validation and comparison of the temperature-based statistics over a region with a complex topography, only a limited number of stations (i.e., a total of 266) could be used in this study. This investigation might be expanded over much larger areas, perhaps executed globally using all available meteorological station-based observations, although the performance of both model- and remote sensing-based products may vary over complex and non-complex regions.

Declarations

Ethical Approval

Not applicable.

Consent to Participate

Not applicable.

Consent to Publish

Not applicable.

Authors Contributions

The author confirms sole responsibility for the conception and methodology, data collection, analysis and interpretation of results, and manuscript writing.

Funding

The author did not receive support from any organization for the submitted work.

Competing Interests

The author has no relevant financial or non-financial interests to disclose.

Availability of data and materials

Datasets from MGM analyzed in this study were provided by MGM on request by the author's institution. Publicly available datasets from ECMWF analyzed in this study can be found here: [https://cds.climate.copernicus.eu/]. Publicly available datasets from NASA analyzed in this study can be found here: [https://e4ftl01.cr.usgs.gov/].

References

Abbasnia M, Toros H (2020) Trend analysis of weather extremes across the coastal and non-coastal areas (case study: Turkey). J Earth Syst Sci 129:. https://doi.org/10.1007/s12040-020-1359-3

Aguilar-Lome J, Espinoza-Villar R, Espinoza JC, et al (2019) Elevation-dependent warming of land surface temperatures in the Andes assessed using MODIS LST time series (2000–2017). Int J Appl Earth Obs Geoinf 77:119–128. https://doi.org/10.1016/j.jag.2018.12.013

790 Amatulli G, Domisch S, Tuanmu MN, et al (2018) Data Descriptor: A suite of global, cross-
791 scale topographic variables for environmental and biodiversity modeling. Sci Data 5:1–
792 15. https://doi.org/10.1038/sdata.2018.40
793 Amjad M, Yilmaz MT, Yucel I, Yilmaz KK (2020) Performance evaluation of satellite- and
794 model-based precipitation products over varying climate and complex topography. J
795 Hydrol 584:124707. https://doi.org/10.1016/j.jhydrol.2020.124707
796 Bagcaci SC, Yucel I, Duzenli E, Yilmaz MT (2021) Intercomparison of the expected change in
797 the temperature and the precipitation retrieved from CMIP6 and CMIP5 climate
798 projections: A Mediterranean hot spot case, Turkey S. Atmos Res 256:105576.
799 https://doi.org/10.1016/j.atmosres.2021.105576
800 Basu R, Samet JM (2002) Relation between elevated ambient temperature and mortality: A
801 review of the epidemiologic evidence. Epidemiol Rev 24:190–202.
802 https://doi.org/10.1093/epirev/mxf007
803 Beck HE, Zimmermann NE, McVicar TR, et al (2018) Figshare.
804 https://doi.org/https://doi.org/10.6084/m9.figshare.6396959
805 Benali A, Carvalho AC, Nunes JP, et al (2012) Estimating air surface temperature in Portugal
806 using MODIS LST data. Remote Sens Environ 124:108–121.
807 https://doi.org/10.1016/J.RSE.2012.04.024
808 CDS Climate Data Store. ECMWF Copernicus. https://cds.climate.copernicus.eu/%0A.
809 Accessed 1 Aug 2022
810 Cos J, Doblas-Reyes F, Jury M, et al (2022) The Mediterranean climate change hotspot in the

811 CMIP5 and CMIP6 projections. Earth Syst Dyn 13:321–340. https://doi.org/10.5194/esd-
812 13-321-2022
813 Duan SB, Li ZL, Leng P (2017) A framework for the retrieval of all-weather land surface
814 temperature at a high spatial resolution from polar-orbiting thermal infrared and passive
815 microwave data. Remote Sens Environ 195:107–117.
816 https://doi.org/10.1016/j.rse.2017.04.008
817 Duan SB, Li ZL, Tang BH, et al (2014) Generation of a time-consistent land surface
818 temperature product from MODIS data. Remote Sens Environ 140:339–349.
819 https://doi.org/10.1016/j.rse.2013.09.003
820 ECMWF (2016) Part IV: Physical Processes. Reading, UK
821 Eken M, Ceylan A, Taştekin AT, et al (2008) Klimataloji-II.
822 https://www.mgm.gov.tr/FILES/genel/kitaplar/klimatoloji2.pdf. Accessed 19 Aug 2022
823 Friedl MA (2002) Forward and inverse modeling of land surface energy balance using surface
824 temperature measurements. Remote Sens Environ 79:344–354
825 Gumus B, Oruc S, Yucel I, Yilmaz MT (2023) Impacts of Climate Change on Extreme Climate
826 Indices in Türkiye Driven by High-Resolution Downscaled CMIP6 Climate Models.
827 Sustain 15:. https://doi.org/10.3390/su15097202
828 Hulley G, Freepartner R, Malakar N, Sarkar S (2022) Moderate Resolution Imaging
829 Spectroradiometer (MODIS) Land Surface Temperature and Emissivity Product (MxD21)
830 User Guide Collection 6.1
831 Imhoff ML, Zhang P, Wolfe RE, Bounoua L (2010) Remote sensing of the urban heat island

effect across biomes in the continental USA. Remote Sens Environ 114:504–513. https://doi.org/10.1016/J.RSE.2009.10.008

IPCC (2021a) Summary for Policymakers. In: Climate Change 2021: The Physical Science Basis. Contribution of Working Group to the Sixth Assessment Report of the Intergovernmental Panel on Climate Change. Cambridge University Press, Cambridge, United Kingdom and New York, NY, USA

IPCC (2023) SYNTHESIS REPORT OF THE IPCC SIXTH ASSESSMENT REPORT (AR6) Summary for Policymakers

IPCC (2021b) Regional factsheet – Europe. Sixth Assessment Report of the Intergovernmental Panel on Climate Change. Working Group I – The Physical Science Basis. https://www.ipcc.ch/report/ar6/wg1/downloads/factsheets/IPCC_AR6_WGI_Regional_Fact_Sheet_Europe.pdf. Accessed 19 Aug 2022

Li ZL, Tang BH, Wu H, et al (2013) Satellite-derived land surface temperature: Current status and perspectives. Remote Sens Environ 131:14–37. https://doi.org/10.1016/j.rse.2012.12.008

Liu J, Hagan DFT, Holmes TR, Liu Y (2022) An Analysis of Spatio-Temporal Relationship between Satellite-Based Land Surface Temperature and Station-Based Near-Surface Air Temperature over Brazil. Remote Sens 14:. https://doi.org/10.3390/rs14174420

Manesh MB, Khosravi H, Alamdarloo EH, et al (2019) Linkage of agricultural drought with meteorological drought in different climates of Iran. Theor Appl Climatol 138:1025–1033. https://doi.org/10.1007/s00704-019-02878-w

MGM İstasyon Bilgileri Veritabanı. T.C. Tarım ve Orman Bakanlığı Meteoroloji Genel Müdürlüğü. https://mgm.gov.tr/kurumsal/istasyonlarimiz.aspx. Accessed 19 Aug 2022

Mildrexler DJ, Zhao M, Running SW (2011) A global comparison between station air temperatures and MODIS land surface temperatures reveals the cooling role of forests. J Geophys Res Biogeosciences 116:1–15. https://doi.org/10.1029/2010JG001486

Muñoz-Sabater J, Dutra E, Agustí-Panareda A et al. (2021) ERA5-Land: A state-of-the-art global reanalysis dataset for land applications. Earth Syst Sci Data 13:4349–4383. https://doi.org/10.5194/essd-13-4349-2021

NASA The Land Processes Distributed Active Archive Center (LP DAAC). https://lpdaac.usgs.gov/data/. Accessed 1 Dec 2022

Njoku EA, Akpan PE, Effiong AE, Babatunde IO (2023) The effects of station density in geostatistical prediction of air temperatures in Sweden: A comparison of two interpolation techniques. Resour Environ Sustain 11:100092. https://doi.org/10.1016/j.resenv.2022.100092

NOAA Global Time Series. https://www.ncei.noaa.gov/access/monitoring/climate-at-a-glance/global/time-series/globe/land_ocean/12/1/2001-2020. Accessed 6 Jun 2023

Pepin N, Deng H, Zhang H, et al (2019) An Examination of Temperature Trends at High Elevations Across the Tibetan Plateau: The Use of MODIS LST to Understand Patterns of Elevation-Dependent Warming. J Geophys Res Atmos 124:5738–5756. https://doi.org/10.1029/2018JD029798

Pepin N, Maeda EE, Williams R (2016) Use of remotely sensed land surface temperature as a

874 proxy for air temperatures at high elevations: Findings from a 5000m elevational transect
875 across Kilimanjaro. J Geophys Res Atmos 121:9998–10015
876 Recondo C, Corbea-Pérez A, Peón J, et al (2022) Empirical Models for Estimating Air
877 Temperature Using MODIS Land Surface Temperature (and Spatiotemporal. Remote
878 Sens 14:3206
879 Reiners P, Asam S, Frey C, et al (2021) Validation of avhrr land surface temperature with modis
880 and in situ lst—a timeline thematic processor. Remote Sens 13:1–30.
881 https://doi.org/10.3390/rs13173473
882 Reiners P, Sobrino J, Kuenzer C (2023) Satellite-Derived Land Surface Temperature Dynamics
883 in the Context of Global Change—A Review. Remote Sens 15:1857.
884 https://doi.org/10.3390/rs15071857
885 Stefanidis K, Varlas G, Papaioannou G, et al (2022) Trends of lake temperature, mixing depth
886 and ice cover thickness of European lakes during the last four decades. Sci Total Environ
887 830:154709. https://doi.org/10.1016/j.scitotenv.2022.154709
888 Vose RS, Menne MJ (2004) A method to determine station density requirements for climate
889 observing networks. J Clim 17:2961–2971. https://doi.org/10.1175/1520-
890 0442(2004)017<2961:AMTDSD>2.0.CO;2
891 Wan Z (2019) Collection-6 MODIS Land Surface Temperature Products Users' Guide
892 Wang YR, Hessen DO, Samset BH, Stordal F (2022) Evaluating global and regional land
893 warming trends in the past decades with both MODIS and ERA5-Land land surface
894 temperature data. Remote Sens Environ 280:. https://doi.org/10.1016/j.rse.2022.113181

WMO (2008) Guide to Hydrological Practice Volume I Hydrology – From Measurement to Hydrological Information (WMO-No. 168). https://library.wmo.int/doc_num.php?explnum_id=10473. Accessed 22 Sep 2022

Yang YZ, Cai WH, Yang J (2017) Evaluation of MODIS land surface temperature data to estimate near-surface air temperature in Northeast China. Remote Sens 9:1–19. https://doi.org/10.3390/rs9050410

Yao R, Wang L, Huang X, et al (2017) Temporal trends of surface urban heat islands and associated determinants in major Chinese cities. Sci Total Environ 609:742–754. https://doi.org/10.1016/j.scitotenv.2017.07.217

Yao R, Wang L, Huang X, et al (2019) Greening in Rural Areas Increases the Surface Urban Heat Island Intensity. Geophys Res Lett 46:2204–2212. https://doi.org/10.1029/2018GL081816

Yao R, Wang L, Huang X, et al (2021) A Robust Method for Filling the Gaps in MODIS and VIIRS Land Surface Temperature Data. IEEE Trans Geosci Remote Sens 59:10738–10752. https://doi.org/10.1109/TGRS.2021.3053284

Yao R, Wang L, Huang X, et al (2023) Global seamless and high-resolution temperature dataset (GSHTD), 2001–2020. Remote Sens Environ 286:113422. https://doi.org/10.1016/j.rse.2022.113422

Yao R, Wang L, Wang S, et al (2020) A detailed comparison of MYD11 and MYD21 land surface temperature products in mainland China. Int J Digit Earth 13:1391–1407. https://doi.org/10.1080/17538947.2019.1711211

916 Yilmaz M (2023) Accuracy assessment of temperature trends from ERA5 and ERA5-Land. Sci
917 Total Environ 856:159182. https://doi.org/10.1016/J.SCITOTENV.2022.159182
918 Yilmaz M (2022) Verification of ERA5 Hourly Air Temperature Data over Turkey. J Nat
919 Hazards Environ 8:207–220. https://doi.org/10.21324/dacd.1001820
920 Zhang H, Zhang F, Zhang G, et al (2016) Evaluation of cloud effects on air temperature
921 estimation using MODIS LST based on ground measurements over the Tibetan Plateau.
922 Atmos Chem Phys 16:13681–13696. https://doi.org/10.5194/acp-16-13681-2016
923 Zhao W, He J, Wu Y, et al (2019) An Analysis of Land Surface Temperature Trends in the
924 Central Himalayan Region Based on MODIS Products. Remote Sens 11:.
925 https://doi.org/10.3390/rs11080900
926
927